

# Degree Course Life Technologies

Major: Biotechnology

# Diploma 2014

- *confidential* -

*Loric Petruzzi*

*Catalytic performance and  
enantioselectivity of  
engineered oxidoreductases as  
biocatalysts*

- *Professor*  
Marc Pfeifer
- *Expert*  
Prof. Stefan Lutz
- *Submission date of the report*  
25.08.2014

SI	TV
X	X

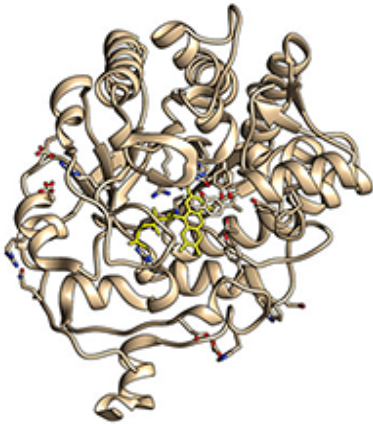
<input type="checkbox"/> FSI <input checked="" type="checkbox"/> FTV	Année académique / Studienjahr 2013/2014	No TD / Nr. DA bt/2014/26
Mandant / Auftraggeber <input type="checkbox"/> HES—SO Valais <input type="checkbox"/> Industrie <input checked="" type="checkbox"/> Ecole hôte	Etudiant / Student Loric Petruzzi	Lieu d'exécution / Ausführungsort <input type="checkbox"/> HES—SO Valais <input type="checkbox"/> Industrie <input checked="" type="checkbox"/> Ecole hôte
Professeur / Dozent Marc Pfeifer	Expert / Experte (données complètes) Prof. Stefan Lutz Department of Chemistry Emory University 1515 Dickey Drive Atlanta, GA 30322 USA	
Travail confidentiel / vertrauliche Arbeit <input checked="" type="checkbox"/> oui / ja <sup>1</sup> <input type="checkbox"/> non / nein		

Titre / Titel <p style="text-align: center;"><b>Catalytic performance and enantioselectivity of engineered oxidoreductases as biocatalysts</b></p>
Description et Objectifs / Beschreibung und Ziele <p>The thesis project will focus on the evaluation of novel biocatalysts for the asymmetric reduction of bioactive compounds with a particular emphasis on terpenoids and fragrances. More specifically, the study will be evaluating the catalytic activity and enantioselectivity of native Old Yellow Enzyme (OYE) from <i>Saccharomyces pastorianus</i> in comparison with three engineered enzyme variants: OYE1(W116I) (Padhi et al. 2009), cpOYE303 (Daugherty et al. 2013) and cpOYE303(W116I) (Lutz, unpublished results).</p> Objectives:

Délais / Termine	
Attribution du thème / Ausgabe des Auftrags: 28.04.2014	Exposition publique / Ausstellung Diplomarbeiten: -
Fin des travaux de diplôme dans les laboratoires de l'école / Ende der Diplomarbeiten in den Labors der Schule: -	Défense orale / Mündliche Verteidigung: à définir
Remise du rapport / Abgabe des Schlussberichts: Au plus tard le 03.11.2014   12h00	
Signature ou visa / Unterschrift oder Visum	
Responsable de la filière Leiter des Studiengangs: 	Etudiant/Student: 

<sup>1</sup> Par sa signature, l'étudiant-e s'engage à respecter strictement la directive et le caractère confidentiel du travail de diplôme qui lui est confié et des informations mises à sa disposition.  
 Durch seine Unterschrift verpflichtet sich der Student, die Richtlinie einzuhalten sowie die Vertraulichkeit der Diplomarbeit und der dafür zur Verfügung gestellten Informationen zu wahren.

# Catalytic performance and enantioselectivity of engineered oxidoreductases as biocatalysts



Petruzzi Loric

## Objectives

The thesis will evaluate the catalytic activity and enantioselectivity of native Old Yellow Enzyme from *S.pastorianus* in comparison with three engineered enzyme variants. Substrates will be bioactive compounds with a particular emphasis on terpenoids and fragrances.

## Methods | Experiences | Results

Three variants and wild type (WT, shown figure up left) Old Yellow Enzyme (OYE) from *S.pastorianus* (OYE1) were used. One mutant, W116I, contained a site-directed mutation that changed Trp-116 to Ile. The active site volume was increased and resulted in a reversed enantioselectivity for (S)-carvone compared to WT OYE1. Then, cp303 was modified by circular permutation. The N- and C-termini were changed but the overall amino acid sequence was kept. The flexibility of the enzyme was increased as well as the size of active site entrance (see figure bottom right). Previous studies showed faster catalytic rates. The last mutant, cp303W116I, is an OYE that combined both peptide alterations (no published results). The enzymes were purified from transformed *E.coli* by Anion Exchange Chromatography and Size Exclusion Chromatography. Enzymatic assays were done in 200  $\mu$ L final volume with 1  $\mu$ M enzyme using 1  $\mu$ M phosphite dehydrogenase and 10 mM sodium phosphite as a regenerating system and 100  $\mu$ M NADP<sup>+</sup> as cofactor. Time points were taken by extracting substrates with organic solvent before being analyzed by chiral GC with an optimized method. Results showed that for rigid linear substrates, mutants were not efficient, showing no enantioselectivity switch or increase in catalytic rates. It was hypothesized that these molecules needed more stabilization in the active site in order to be efficiently catalyzed. However, mutants showed high rates with (S/R)-carvone.

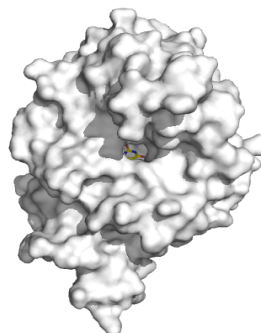
Bachelor's Thesis  
| 2014 |

Degree course  
*Life Technologies*

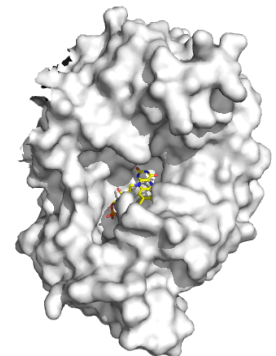
Field of application  
*Biotechnology*

Supervising professor  
Dr. Pfeifer Marc  
[marc.pfeifer@hevs.ch](mailto:marc.pfeifer@hevs.ch)

Partner  
Prof. Lutz Stefan  
Emory University  
[sal2@emory.edu](mailto:sal2@emory.edu)



Crystal structure of wild type Old Yellow Enzyme from *S.pastorianus*. In the middle is the entrance of the active site with the FMN cofactor in yellow.



Crystal structure of cp303 mutant of the Old Yellow Enzyme from *S.pastorianus*. In the middle is shown the increased entry of the active site.

This document is the original report written by the student.  
It wasn't corrected and may contain inaccuracies and errors.



***“Learn from yesterday, live for today, hope for tomorrow.  
The important thing is not to stop questioning.”***

*Albert Einstein*

## Table of contents

<b>1. Abbreviations</b> .....	<b>4</b>
<b>2. Introduction</b> .....	<b>5</b>
<b>3. Project objectives</b> .....	<b>10</b>
<b>4. Material and methods</b> .....	<b>11</b>
4.1 Material .....	11
4.1.1 Equipment .....	11
4.1.2 Cells .....	11
4.1.3 Reagents .....	12
4.1.4 Softwares .....	14
4.2 Methods .....	15
4.2.1 Cell transformation by electroporation .....	15
4.2.2 Overexpression of cp303W116I and W116I .....	16
4.2.3 Purification of cp303W116I and W116I from E.coli BL21(DE3) by anion exchange chromatography .....	16
4.2.4 Size exclusion chromatography .....	17
4.3 Estimating purity with SDS-PAGE .....	19
4.4 Determination of purified enzyme concentration .....	20
4.5 Enzymatic Assays .....	21
4.5.1 Calculations of relatives concentrations .....	22
4.5.2 Calculation of enantiomeric excess .....	22
4.5.3 Calculation of conversion rates .....	22
4.6 Gas Chromatography analysis .....	23
4.6.1 ( <i>S/R</i> )-carvone .....	25
4.6.2 Trans $\alpha$ -methyl-cinnamaldehyde .....	25
4.6.3 Myrtenol .....	25
4.6.4 Methyl 2-hydroxymethylacrylate .....	25
4.6.5 4-phenyl-3-butyn-2-one .....	25
4.6.6 ( <i>E/Z</i> )-citral .....	25
<b>5. Results</b> .....	<b>26</b>
5.1 Enzyme purification .....	26
5.2 Calculation of enzyme concentration .....	26

5.3	Catalytic rate and enantioselectivity of mutants .....	27
5.3.1	( <i>S</i> )-carvone .....	27
5.3.2	( <i>R</i> )-carvone .....	28
5.3.3	Trans $\alpha$ -methyl-cinnamaldehyde .....	29
5.3.4	Myrtenol .....	31
5.3.5	Methyl 2-hydroxymethylacrylate .....	33
5.3.6	4-phenyl-3-butyn-2-one .....	35
5.3.7	( <i>E/Z</i> )-Citral .....	37
<b>6.</b>	<b>Discussion .....</b>	<b>42</b>
6.1	( <i>S</i> )-carvone .....	42
6.2	( <i>R</i> )-carvone .....	43
6.3	Trans $\alpha$ -methylcinnamaldehyde .....	44
6.4	Myrtenol .....	45
6.5	Methyl 2-hydroxymethylacrylate .....	46
6.6	4-phenyl-3-butyn-2-one .....	46
6.7	( <i>E/Z</i> )-citral .....	47
<b>7.</b>	<b>Conclusion .....</b>	<b>48</b>
<b>8.</b>	<b>Acknowledgements .....</b>	<b>49</b>
<b>9.</b>	<b>Literature .....</b>	<b>50</b>
<b>10.</b>	<b>Appendix .....</b>	<b>53</b>
10.1	Recipes for reagent used during the experiment .....	53
10.2	Anion Exchange Chromatography .....	55
10.3	Size Exclusion Chromatography .....	56
10.4	Relatives concentrations and quantitative additional data .....	57
10.4.1	( <i>S</i> )-carvone .....	57
10.4.2	( <i>R</i> )-carvone .....	59
10.4.3	Trans $\alpha$ -methyl-cinnamaldehyde .....	61
10.4.4	Methyl 2-hydroxymethylacrylate .....	63
10.4.5	4-phenyl-3-butyn-2-one .....	64
10.4.6	( <i>E/Z</i> )-citral .....	66
10.5	Equipment pictures .....	68
10.5.1	Anion and Size exclusion Äkta module .....	68
10.5.2	Gas Chromatography .....	69
10.5.3	Anaerobical chamber .....	70

## 1. Abbreviations

Index of the abbreviations used in the text listed in alphabetical order.

AEX	Anion Exchange Chromatography
CP	Circular Permutation
cp303	OYE Circular Permutant n°303 from <i>Daugherty et al.</i> [1] study
cp303W116I	OYE Circular Permutant plus tryptophan mutant
CV	Column Volume
DMSO	Dimethyl sulfoxide
DNA	Deoxyribonucleic acid
<i>E. coli</i>	<i>Escherichia coli</i>
EWG	Electron Withdrawing Group
FAD	Flavin Adenine Dinucleotide
FID	Flame Ionization Detector
FMN	Flavin Mononucleotide
GC	Gas Chromatography
IPTG	$\beta$ -D-1-thiogalactopyranoside
kDa	Kilo Daltons
LB	Lysogeny Broth
MeOH	Methanol
NADP	Nicotinamide Adenine Dinucleotide
NaPi	Sodium phosphite
OYE	Old Yellow Enzyme
OYE1	Old Yellow Enzyme from <i>S.pastonarius</i>
PCR	Polymerase Chain Reaction
PTDH	Phosphite dehydrogenase
RT	Room Temperature
<i>S.cerevisiae</i>	<i>Saccharomyces cerevisiae</i>
SEC	Size Exclusion Chromatography
SDS	Sodium Dodecyl Sulfate
SDS-PAGE	Polyacrylamide Gel Electrophoresis in presence of SDS
<i>S.pastonarius</i>	<i>Saccharomyces pastonarius</i>
W116I	OYE tryptophan mutant from <i>Padhi et al.</i> [2] study
WT	Wild Type OYE1

## 2. Introduction

Nowadays, enzyme mediated biotransformations, which are chemical modifications involving a biological catalyst, are very useful and helpful processes. These have several advantages compared to chemical transformations, like remarkable chemo-, regio- and stereoselectivity and mild reaction conditions (temperature, pH). These properties meet the growing demand for sustainable and cost effective “green chemistry” processes.

Removing or adding an electron to a molecule belongs to the so-called redox reactions. It is one of the most investigated topics in biocatalysts research because it may lead to the creation of a chiral center. This is happening when the four substituents of a tetrahedral atom (usually carbon) are different. There are two possible dispositions of the substituents in space per each chiral center. One is the R and the other is the S-enantiomer, depending on the relative position of the substituents. These molecules have the same formula and atoms composition. The only detail that differs is the disposition of the substituents around a chiral center, which cause them to be the mirror image of each other, like the right and the left hand are. All biologically active molecules are chiral, and so are the majority of today's drugs [3].

Two enantiomers have similar chemical and physical properties. However, it is known that their effect as drug may be different depending on their different conformation. Thalidomide [4], Naproxen [5] or L- $\alpha$ -methyl dopa [6] are good examples of why producing enantiopure drugs has become a real concern. Enantiomers, obtained by bioreduction, like the Roche-Ester [7, 8], may also be used as starting material for several industrially relevant molecules like vitamins, fragrance compounds, antibiotics or natural products.

Today's helpful molecules are becoming more and more complex, because of the increasing number of chiral centers they feature. As seen before, classic chemistry cannot be as efficient as biocatalysts in creating enantiopure solutions. Biocatalysis is where the enzymes like the ones from the Old Yellow Enzyme (OYE) family found their usefulness. This kind of enzyme is able to reduce activated alkenes, which are organic molecules containing a double bonds and an electron withdrawing group (EWG) that weaken the double bond. The electron transfer is done with the help of a cofactor incorporated in the OYE, which can be: a flavin mononucleotide (FMN), a flavin adenine dinucleotide (FAD) or a nicotinamide adenine dinucleotide (NAD(P)). Enzymes are generally efficient for one or a group of substrates. Frequently, the enzyme can only either slightly catalyze, or not catalyze at all, the target molecule for which it is not adapted. Because of this, the enzyme must be optimized.

Today, thanks to protein engineering it is possible to modify the amino acids sequence of enzymes in order to affect (i.e. improve) their characteristics like their selectivity, their activity or even their physicochemical characteristics. The purpose of these modifications is to enhance those small catalytic units in order to optimize processes or investigate new synthetic pathways for industrially relevant molecules. Usually, changes of enzymatic properties have been recently achieved with different techniques, which can be divided into two approaches: rational design and directed evolution. Rational design is based on pre-acquired knowledge and focused on deleting, substituting or re-arranging one or several amino acids within the protein sequence.

Instead, the aim of directed evolution is to try to mimic the effect of evolution on several thousand years by using molecular biology and applying a selective pressure to find enzyme with improved properties. The effect of these changes within enzyme's structure are difficult to predict [9] but, it is possible to study them through techniques such as crystallography and biophysical methods.

Recently, a new approach of protein engineering, the circular permutation (CP), has been introduced. It is based on the modification of the tertiary structure of an enzyme by re-arranging the overall amino acid composition. That means that the overall amino acids composition do not change but the N and C-termini are located elsewhere [1].

The aim of this work is to study the substrate and enantioselectivity of the native OYE from *Saccharomyces pastonarius* and three variants obtained by protein engineering. Wild Type OYE1 (WT) is 400 amino acids long and weights 40 kDa. The active site is showed in figure 1 where eight amino acid side chains are highlighted: Thr-37, Trp-116, His-191, Tyr-196, Asn-194, Phe-250, Phe-296 and Tyr-375. Most of them are contributing to create a hydrophobic environment in the pocket, while others have a bigger importance. Indeed, Massey and Kohli have investigated the role of Tyr-196 [10], it was suggested that tyrosine 196 helps with the proton transfer during the oxidative half-reaction with the reduced flavin and an activated alkene. Massey also studied the role of asparagine 194 and histidine 191 [11]. Those residues were identified to make hydrogen bonds with phenolic compounds in order to stabilize them in the active site.

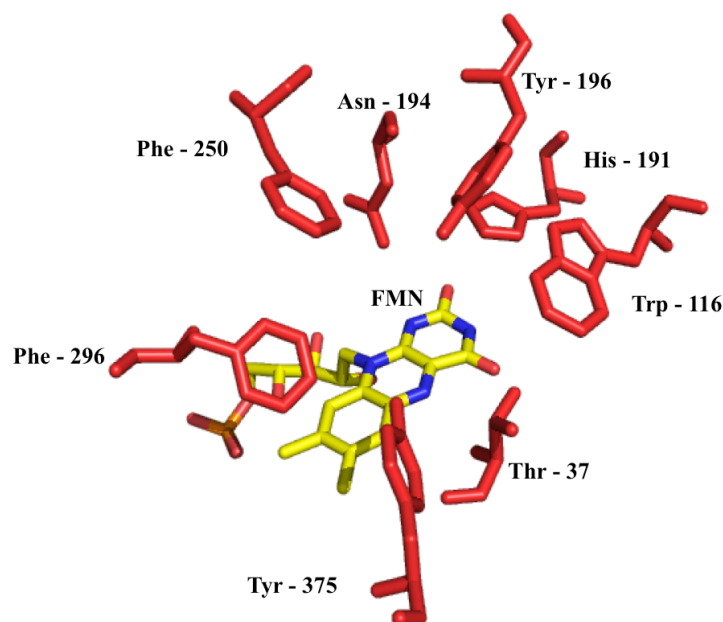


**Figure 1:** Active site of the Wild Type Old Yellow Enzyme 1 (OYE1) from *S.pastonarius*. Some amino acids that take part to the formation of the active site are highlighted in red. They are close to where the substrate binds with the FMN, which is shown on the bottom of the active site pocket.

The first mutant, W116I, has been modified by site-directed mutagenesis. The tryptophan in position 116 was replaced by an isoleucine [2] (Trp is showed on the middle right of figure 1). This variant was chosen because it showed a change in enantioselectivity by producing enantiomeric products from the reduction of (*S*)-carvone instead of diastereoisomeric products [2]. *Padhi et al.*[2] made the assumption that replacing Trp by Ile permit a new orientation of the (*S*)-carvone into the active site and also increased its volume by allowing the access to a hydrophobic pocket.

The second variant is the cp303 and was modified by circular permutation. CP was done with a tandem of two attached enzyme genes (*oye1* in the figure 2), which were linked with a tri-peptide. Then, with a polymerase chain reaction (PCR) technique, it was possible to create various mutants by selecting a beginning and an end at different positions on the tandem. The trick resides in designing primers that will always give a fragment of the same length (figure 2). Therefore, the overall amino acids composition is kept.

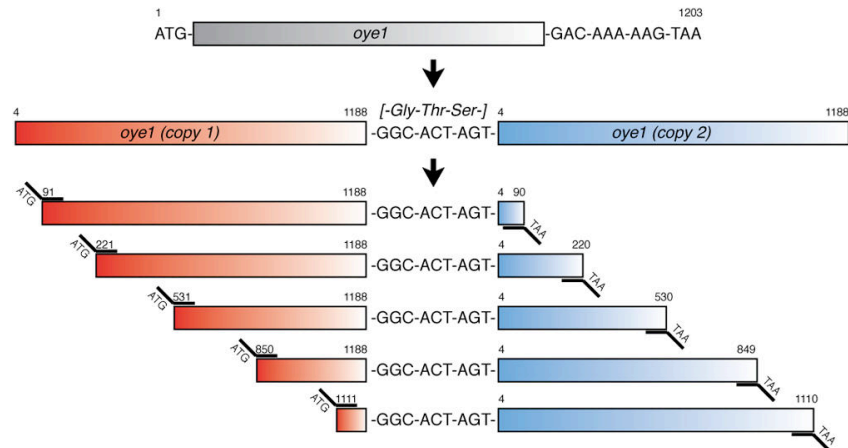


**Figure 2:** Creation of circular permutants of *OYE1* [1]. The two genes are plugged together with a nine-nucleotide sequence encoding the -Gly-Thr-Ser- linker. PCR amplification with site-specific primers will give different fragments of same length each (1188 nucleotides) but with different N and C-termini. Picture from Daugherty et al [1].

One of the variants (cp303) thus obtained was showing significant improvement in activity for (*S*)-carvone and ketoisophorone, up to 10 fold higher than the wild type [1]. Statements were that removing the loop containing Phe-296 (figure 1) resulted in a significantly higher oxidative half reaction rate and in a better flexibility of the enzyme [1]. The opening to the active site was enlarged, as it is possible to see in figure 3.

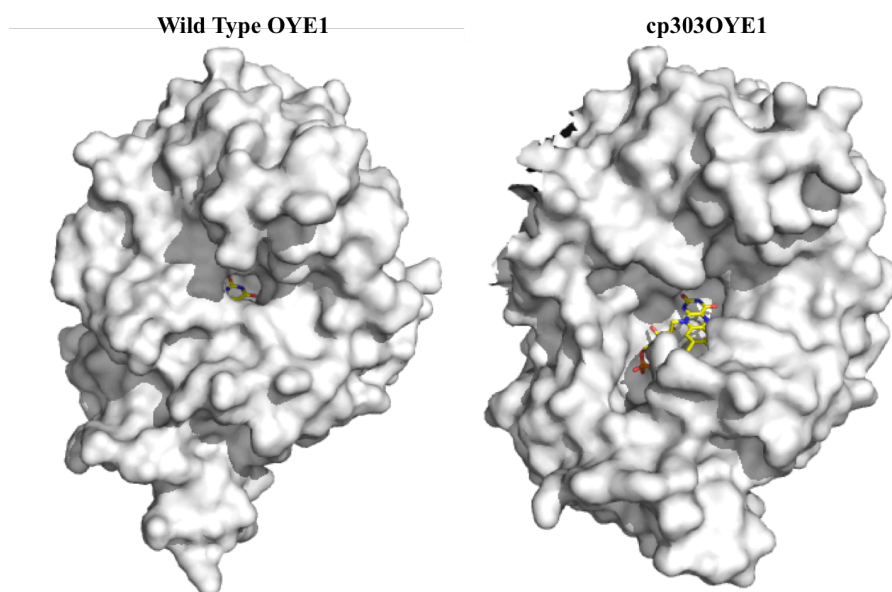


**Figure 3:** Comparison of the active site entrance between the WT and the circular permuted one. A FMN molecule is shown in the bottom of the pocket.

The last mutant, cp303W116I is a variant containing the tryptophan mutation as well as the same N and C-termini as cp303 (unpublished results). This last mutant was produced assuming it will have additives properties with the effect of the site directed mutagenesis as well as the circular permutation.

In order to investigate the previous statements made on each OYE1 variant, different substrates with unique properties will be used. (*S/R*)-carvone (***S/R*-1**) are molecules that have an industrial interest in flavors and fragrances industry [12]. Due to their high volatility, (*S*)-carvone reduced products, (*2R,5S*)- or (*2S,5S*)-carvone, respectively (***R/S*-2**) and (***S/S*-2**), are used as inhibitors of bacteria and filamentous fungi repellents [13]. They are also used as starting compounds in the synthesis of bioproducts like antimalarial drugs [14] or valuable chiral synthons (synthetic building blocks) [15, 16]. Carvone is also used as a reference and control because is one of the most common substrate used with OYEs [1, 2, 7]. *Trans*  $\alpha$ -methyl-cinnamaldehyde (**3**) is a conjugated system, which (*S/R*)- $\alpha$ -methyl-dihydrocinnamaldehyde, (***S/R*-4**) are molecules with an industrial relevance for perfumery as starting material for fragrance compounds [17-19]. Myrtenol (**5**) is a fragrance component used in decorative cosmetics (fine fragrance, shampoos, soaps, etc.) as well as in non-cosmetic products like detergents or household cleaners [20]. Unlike the others molecules used in this work, myrtenol is not a flat component because it contains a bicyclic structure. Because the modifications made on the active site of OYE1 [1, 2], it is expected that one of the variants will be able to process that bulky substrate. Bioreduction of methyl-2-hydroxymethylacrylate (**7**) was investigated with OYE1 variants because that leads to (*R*)-Roche-Ester, (***R*-8**), which is a popular chiral building block for the synthesis of various compounds [7, 8]. It can be used to get vitamins (vitamin E [21]), fragrance molecules (muscone [22]), antibiotics (calcimycin [23]) and other natural products (spiculoic acid [24]) [8]. 4-phenyl-3-butyn-2-one (**9**) contains a triple bond; therefore it is an example for the use of OYE in a reaction that implies two consecutive bioreductions. This molecule was chosen because of the possibility to compare with previous results from BASF [25].

Finally, the (*E/Z*)-Citral, (**E/Z**)-**12**, is another reference substrate as it is a largely used molecule used for bioreductions. Furthermore, **E-12** (geranial) and **Z-12** (neral) forms are two different substrates for OYE. The native OYE1 catalyzes the conversion to the enantiopure products (**E-12** to (*R*)-citronellal, (**R**)-**13** and **Z-12** to (*S*)-citronellal, (**S**)-**13** [26]). Both enantiomers, (**S/R**)-**13** are used in the synthesis of menthol [27].

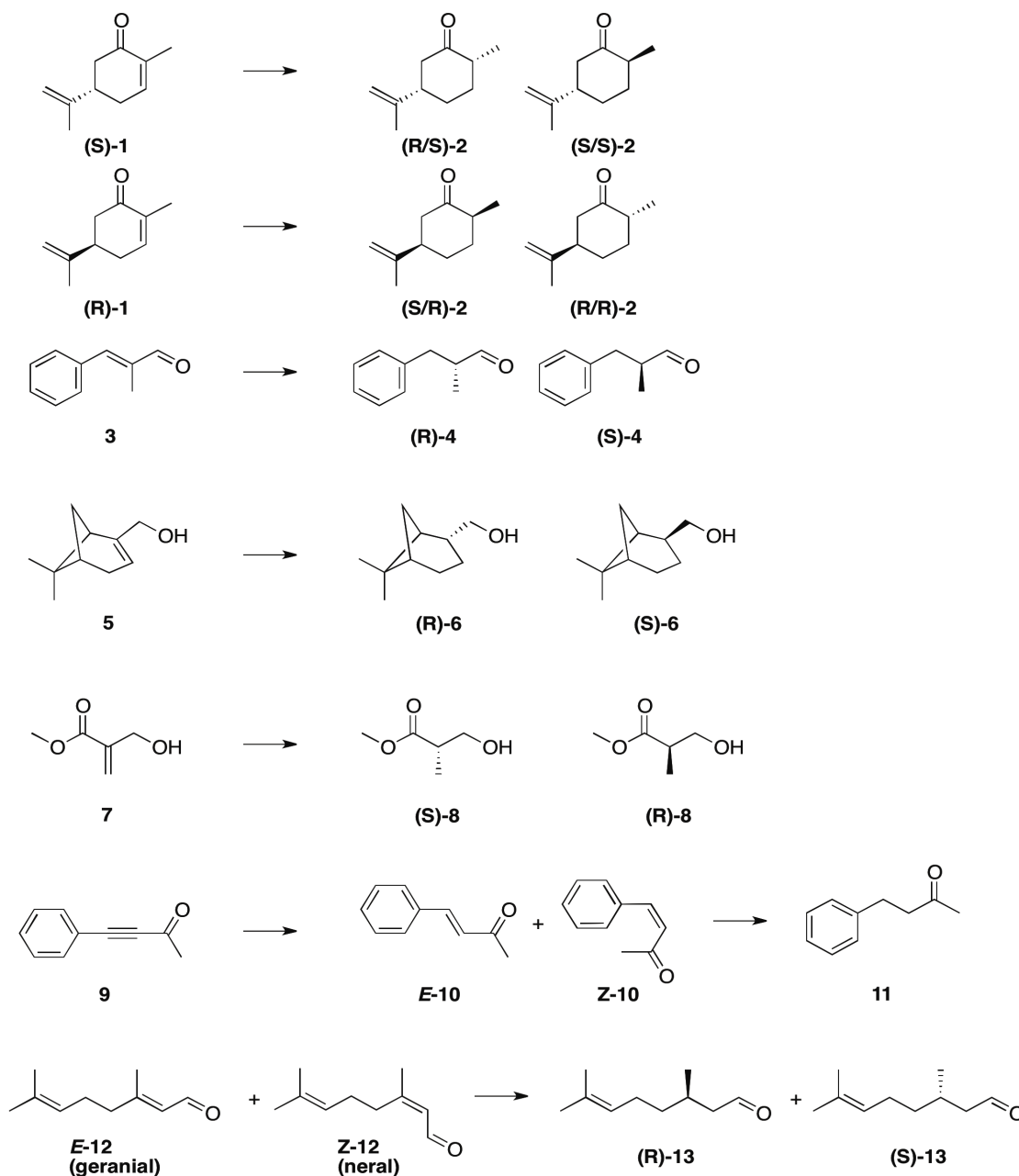


**Figure 4:** Structure of the substrates used in this thesis. (**S/R**)-**1** is (*S/R*)-carvone. (**R/S**)- and (**S/S**)-**2** stands for (*2R,5S*)- and (*2S,5S*)-carvone. **3** is *trans*- $\alpha$ -methylcinnamaldehyde. (**S/R**)-**4** is for (*S/R*)- $\alpha$ -methyl-dihydrocinnamaldehyde. **5** is for myrtenol. (**S/R**)-**6** stands for (*S/R*)-dihydromertanol. **7** is for methyl 2-hydroxymethylacrylate. (**S/R**)-**8** is for (*S/R*)-methyl-3-hydroxy-2-methylpropionate “Roche Ester”. **9** is for 4-phenyl-3-butyne-2-one. (**E/Z**)-**10** is for (*E/Z*)-4-phenyl-3-buten-2-one. **11** is for 4-phenyl-3-butanone. (**E/Z**)-**12** is for (*E/Z*)-citral, respectively geranial and neral. (**S/R**)-**13** is for (*S/R*)-citronellal.

### 3. Project objectives

The goal of this study will be to determine the enantioselectivity and the catalytic activity for wild type OYE1 and three engineered variants among a set of various substrates.

Previous work by *Padhi et al.* [2] led to development of the W116I mutant, after it was observed that WT was presenting diminished rates for 3-ethyl-2-cyclohexanone (figure 5). It was believed that these lower rates were a consequence of unfavorable steric interactions within the active site. In order to reduce these interactions, the active site volume was increased. Amino acids residues that were closest to the active site were investigated and attention was focused on residues that were within a distance of 5 Å of where the substrate binds. Relying on previous studies by Massey [10, 11, 28], the known amino acids that are essential for catalytic purposes were removed from the list. From the remaining amino acids, Trp-116 was chosen because it was the closest to where the  $\beta$ -substituents of 2-cyclohexenone were. Several mutations were made, but the isoleucine mutant was kept. The result on (*S*)-carvone showed a switch in enantioselectivity by producing (2*S*,5*S*)-carvone as major product instead of (2*R*,5*S*)-carvone as the wild type does. However, the mutant was not tested against substrates significantly different than (**S**)-1. This work will try to better understand the features of this new enzyme as well as possible enantioselectivity switch with other substrates.

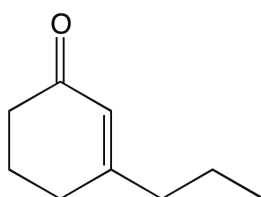


**Figure 5:** 3-ethyl-2-cyclohexenone.

Circular permutation [29] was used by *Daugherty et al.* [1] to create a library of OYE variants. In order to find mutants with a higher activity among the library, OYE circular permutants were synthesized with an in vitro transcription/translation (IVTT) system. This *ex vivo* protein engineering strategy allowed the exploration of a library of hundreds of enzyme variants to highlight the ones with a higher activity. Among the selected enzymes, circular permutant #303 (cp303) was found to have an increased activity, up to > 10x for (*S*)-carvone compared to WT. Further studies showed that cp303 was allowing a faster regeneration of the cofactor. These results were in accordance with previous studies [30] that identified the loop region VI (the truncated region, amino acids from 290 to 310) as taking part in the reductive half reaction. Also, the active site entrance was significantly increased (see figure 3). Through this work, this variant will be tested with different substrates in order to formulate a better understanding of the nature of modifications presented in the cp303 scaffold.

The last variant is an OYE containing the cp303 and the Trp-116 changes. No studies were done on this enzyme before the beginning of this work. It has been suggested that this mutant would show additive properties regarding cp303 and W116I.

Other ongoing studies are investigating alternative amino acids positions for site-directed mutagenesis, such as an Ala instead of Pro-296 (located in the same region as cp303), which showed an increase in conversion rates with (*S*)-carvone by an order of magnitude about 5x higher than WT (Lutz unpublished data based on IVTT system).

## 4. Material and methods

### 4.1 Material

#### 4.1.1 Equipment

**Table 1:** Listing of the specific equipment used for this work.

Model	Provider	Use
GenePulser Xcell	BioRad	Electroporation of competent cells ( <i>E. coli</i> BL21 and DH5 $\alpha$ )
Äkta purifier	Amersham pharmacia biotech	Anion-Exchange Chromatography to purify proteins
HiTrap Q HP 5 ml (34 $\mu$ m bead size, bed dimension 7x25 mm)	GE Healthcare	Anion-Exchange Chromatography
Agilent 6850 series	Agilent Technologies	Gas Chromatography analysis
Cyclosil-B 113-6632, 30 m, film 0.25 $\mu$ M	Agilent Technologies	Gas Chromatography analysis
Sonic Dismembrator Model 100	Fisher Scientific	Cell lysis in purification step
Millex-HV (0.45 $\mu$ m) article: SLHV033RS	Millipore	Clean clear lysate in purification step
Amicon Ultra-15 Centrifugal Filter Device article: UFC901024	Millipore	Concentration of protein before size exclusion separation
HiPrep 16/60 Sephacryl S-100 High resolution 120 ml	GE Healthcare	Size Exclusion Chromatography
Ressource Q 1 ml	Pharmacia Biotech	Anion-Exchange Chromatography
Orbital Shaker S-500	VWR	Enzymatic Assay

#### 4.1.2 Cells

**Table 2:** Listing of cell lines used in this work.

Cell line	Provider	Use
BL21(DE3)pLysS	Invitrogen	Host cell for the transformation and expression of recombinant OYE

### 4.1.3 Reagents

**Table 3:** All reagents and chemicals used for the purpose of this work. Table 1/2.

Substance	Provider / Art. / Lot	Use
Bacto™ Peptone	Becton Dickinson / 211677 / 2012329	2YT medium for protein expression
Yeast Extract	Fisher BioReagents / BP1422 / 121653	2YT medium for protein expression
Sodium Chloride	Macron / 7581 / 0000038485	2YT medium and purification buffers
Tris Hydrochloride 1M Solution pH 8	Fisher BioReagents / BP1758 / 135742	Purification buffers
Benzonase nuclease	Sigma / E1014 / SLBJ7662V	Cell lysis in purification step
Lysozyme	Sigma / L-6876 / 127F-81301	Cell lysis in purification step
Phenylmethylsulfonyl fluoride (PMSF)	Thermo Scientific / 36978 / JL1176862	Cell lysis in purification step
Isopropanol	Fisher Scientific / A451-4 / 115991	SDS-PAGE
SDS 10% solution	Fisher Scientific / BP2436-1 / 044922	SDS-PAGE
Stacking Gel Buffer (0.5 M Tris pH 6.8)	BioRad / 161-0799	SDS-PAGE
Resolving Gel Buffer (1.5 M Tris, pH 8.8)	BioRad / 161-0798	SDS-PAGE
Tetramethylethylenediamine (TEMED)	Fisher BioReagent / BP15020 / 101031	SDS-PAGE
40% Acrylamide/Bis Solution 29 :1	BioRad / 161-0144 / 76782A	SDS-PAGE
Ammonium Persulfate (APS)	Fischer Scientific / 106372 / BP179-25	SDS-PAGE
(S)-carvone	Sigma Aldrich / 435759 / MKBD9582V	Enzymatic Assay
(R)-carvone	Sigma Aldrich / 124931 / 78897MJV	Enzymatic Assay

**Table 4:** All reagents and chemicals used for the purpose of this work. Table 2/2.

<b>Substance</b>	<b>Provider / Art. / Lot</b>	<b>Use</b>
( <i>E/Z</i> )-citral	Sigma Aldrich / C83007 / 7819MJ	Enzymatic Assay
( <i>R</i> )-(+)-citronellal	Aldrich / 343641 / MKBM0881V	GC Reference molecule
( <i>S</i> )-(-)-citronellal	Aldrich / 373753 / BCBJ9098V	GC Reference molecule
<i>trans</i> $\alpha$ -methyl-cinnamaldehyde	Sigma Aldrich / 112275 / 14719JUV	Enzymatic Assay
3-phenylpropionaldehyde	Acros Organics / 24510050 / A0305564	GC Reference molecule
Myrtenol	Wako / 328-53101	Enzymatic Assay
(+)- <i>trans</i> -Myrtanol	Fluka / 70117 / BCBF9640V	GC Reference molecule
4-phenyl-3-butyne-2-one	TCI / P1336 / SAN6M-BJ	Enzymatic Assay
<i>trans</i> 4-phenyl-3-buten-2-one	Acros Organics / 164520500 / A0329138	GC Reference molecule
4-phenyl-2-butanone	Acros Organics / 105830050 / A0102795	GC Reference molecule
Methyl 1-(hydroxymethylacrylate)	Combi-Blocks / QB-2069 / L79180	Enzymatic Assay
Methyl ( <i>R</i> )-(-)- $\beta$ -hydroxyisobutyrate	Acros Organics / 436180010 / 339416	GC Reference molecule
Methyl ( <i>S</i> )-(+)-3-hydroxy-2-methylpropionate	Alfa Aesar / 44483 / D10Z028	GC Reference molecule

#### 4.1.4 Softwares

<b>Name / Version</b>	<b>Developer</b>	<b>Use</b>
Microsoft Excel / 14.3.8	Microsoft	Gas chromatography data analysis, enantiomeric excess and quantitative data calculation
Prism / 6.0e	GraphPad Softwares, Inc.	Conversion rate calculation and figures creation
PyMOL / 1.6.0.0	Schrödinger LLC.	Figures creation
GC ChemStation / B.03.02 [341]	Agilent Technologies	Gas Chromatography analysis

## 4.2 Methods

### 4.2.1 Cell transformation by electroporation

Genes of the targeted OYE1 enzymes have been cloned into a pET14b (4.7 kb) vector. This plasmid contains a T7 expression system as well as an Ampicillin resistance. It allows the induction of the recombinant protein expression by the presence of isopropyl  $\beta$ -D-1-thiogalactopyranoside (IPTG). This molecule binds the lac repressor (see figure 6) and leads to the transcription of the regulated gene. For a proper expression an *E.coli* strain containing the DE3 gene (such as the BL21(DE3)pLysS used in this work), which carries the information to express the T7 RNA polymerase as well as its regulation by the *lac* promoter. This engineered strain of *E.coli* allows an increased stability of the expressed proteins because is deficient in lon and aspartyl proteases. It also contain a pLysS plasmid [31], which is an additional control for the expression of the recombinant gene. It encodes for the T7 lysozyme, which is a natural inhibitor of T7 RNA polymerase [32].

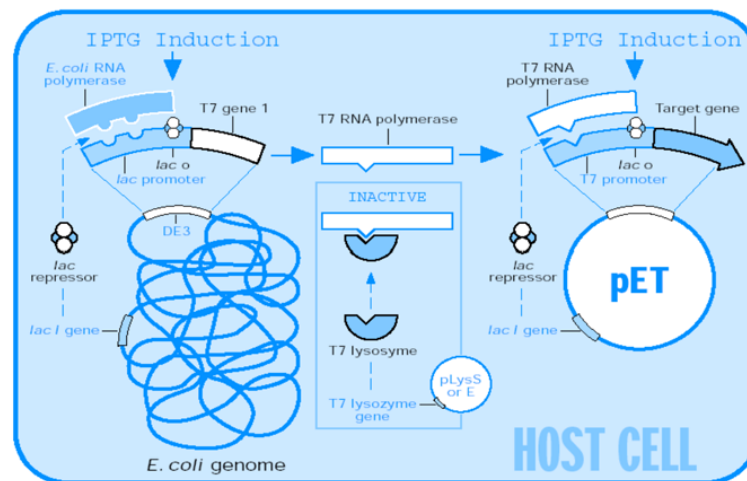


**Figure 6:** Control elements of the pET System [32].

*E.coli* BL21(DE3)pLysS competent cells are transformed with pET14b-cpOYE303W116I and pET14b-OYEW116I by electroporation. 150 ng of DNA is added to 100  $\mu$ L of cells before the suspension is transferred in the electroporation cuvette. The transformation is performed with one pulse (capacitance 25  $\mu$ F, resistance 200  $\Omega$ , 2 mm cuvette) and 1 mL of lysogeny broth (LB, Bacto™ Peptone 10 g/L, Yeats Extract 5 g/L, NaCl 10 g/L at pH 7) is immediately added to the cells and transferred to a sterile Eppendorf. Then, transformed cells are incubated 30 min at 37°C to allow the reconstitution of the membranes and the expression of the genes responsible for the antibiotic resistance. Finally, 200  $\mu$ L are used to inoculate an agar LB plate (containing ampicillin and chloramphenicol), which is incubated overnight at 37°C.

#### 4.2.2 Overexpression of *cp303W116I* and *W116I*

A single colony of transformed *E.coli* BL21 is inoculated in 2 mL of LB with antibiotics (chloramphenicol and ampicillin at 34 µg/ml and 100 µg/ml respectively) and incubated overnight at 37°C. Then, the whole volume is used as inoculum for 600 mL of 2YT (Bacto™ Peptone 16 g/L, Yeast Extract 10 g/L, NaCl 5 g/L at pH 7). This culture is incubated at 37°C with shaking at 200rpm until its optical density at 600nm (OD<sub>600</sub>) reaches 0.5 – 0.7. Overexpression of the recombinant protein is induced by the addition of 1 M IPTG to a final concentration of 0.4 mM for 18 hours at 20°C. After that, the cells are harvested by centrifugation at 4°C for 20 min 4000 g. The cell pellet is washed in 20 mL of buffer A (NaCl 20 mM, Tris-HCl 40 mM at pH 8) in 50 mL Falcon tubes. These tubes are then centrifuged with the same conditions as before. Once the supernatant is removed, the cell pellet can be stored at -20°C.

#### 4.2.3 Purification of *cp303W116I* and *W116I* from *E.coli* BL21(DE3) by anion exchange chromatography

OYE enzymes were purified by anion exchange chromatography (AEX). A clear lysate solution was obtained by sonication, which promotes the disruption of cell membranes by the generation of sonic waves. This phenomenon involves the formation of a vapor phase in a liquid phase, in the same way as boiling does. The difference is that it is not the heat that induces vapor formation but high pressures. The bubbles, or cavities, formed will implode and generate intense shockwaves when subjected to higher pressures [33]. After centrifugation, the clear lysate is harvested and purified through the anion exchange column. The stationary phase is functionalized with quaternary ammonium radicals, -NH<sub>4</sub><sup>+</sup>, which are strong anion exchanger groups (see figure 7). The capture of OYE1 on the column is achieved with the help of negatively charged amino acids (Glu, Asp) regions on the enzyme, which will interact with the positively charged stationary phase. Once the column retains the compound, the system is washed in order to remove from the column non-specific bound molecules. Then, a gradient of a stronger anion competitor (NaCl or KCl) is passed through the system in order to displace the molecules attached to the stationary phase. At the column's end, a spectrophotometric detector that can be set to a desired wavelength analyzes the buffers. The flavin cofactor bound in OYE1 enzymes has two distinct absorbance peaks at 360 and 460 nm; therefore the elution of the enzyme can be easily monitored. In order to follow the presence of the overall proteins, a third wavelength is set at 274 nm.

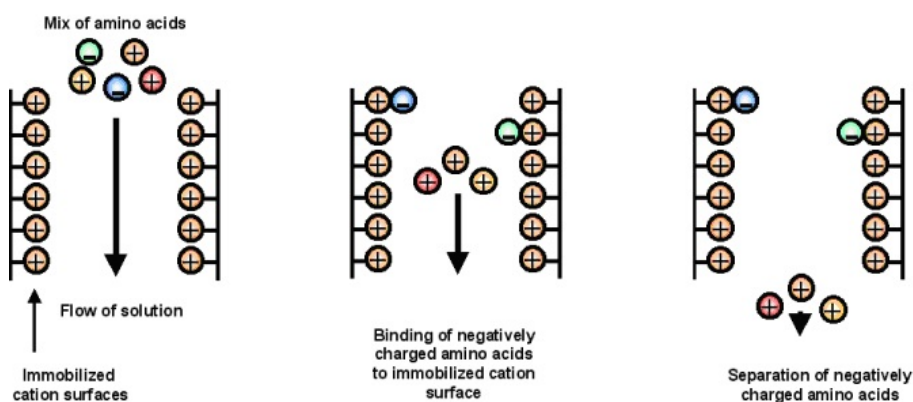


**Figure 7:** Diagram showing the anion exchange chromatography principle. In this experiment, the immobilized cation surface is made of ammonium groups (-NH<sub>4</sub><sup>+</sup>) and the negatively charged balls represents the OYE1.

Cell pellet containing an expressed OYE were suspended with a ratio of 1 g<sub>cells</sub>/6 mL in lysis buffer (1 mM PMSF, 1750 U benzonase nuclease and 10 mg lysozyme in buffer A) and stored on ice for 30 min. Cells were kept in ice and lysed by sonication (9x with 10 s pulse and 20 s pause) and cell extract was then centrifuged at 4°C for 30 min 16100 g. The clear lysate obtained was loaded at 5 mL/min into a pre-equilibrated HiTrap Q FF (5 mL) column with 3 column volumes (CV) of buffer A (Tris-HCl 40 mM at pH 8; depending on the protein concentration, two of those columns could be plugged in series on an Äkta purifier). The column was washed with 2 CV of buffer A until the A<sub>274nm</sub> was stable. The elution of OYE was obtained with a gradient from 0 to 100% in 10 CV of buffer B (1 M NaCl, 40 mM Tris-HCl at pH 8), collecting the peak corresponding to the increase in the absorbance at 360 and 460 nm. The collected fractions were pooled together and concentrated by centrifugation at 4°C for 20 min, 4000 g with an Amicon Ultra-15 Centrifugal Filter Devices by Millipore (molecular weight cut-off: 10 kDa).

#### 4.2.4 Size exclusion chromatography

In order to remove the last contaminants, a size exclusion chromatography (SEC) is performed as final step. This technique is usually used to remove small contaminants in an already purified solution. Through the column, particles will be separated depending on their molecular size. Therefore, it is important to notice that this technique is efficient only for molecules with a significant difference in their size. The column is packed with porous beads through which small molecules will travel (green path on figure 8). Obviously, if a molecule is too large to enter a pore, it will continue to flow through the system without being retained (red path). The result of this is that the small compounds have a higher retention time than the large ones.

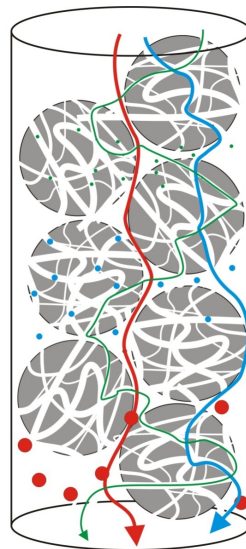


**Figure 8:** Size exclusion chromatography principle. Small particles (green line) will enter porous beads and thus stay longer in the column, while larger molecules (red line) will pass through without being retained.

SEC column efficiency can be visualized with selectivity curves. These graphics are obtained by plotting the elution volume [mL] against the molecular weight [kDa]. The lines can inform the user on the molecular weight range where the column will be efficient. The selectivity curve corresponding to the column used in this work (HiPrep 16/60 Sephacryl S-100 High Resolution) is shown in the figure 9. Knowing that the OYE has an approximate molecular weight of 44 kDa, it should be eluted after 45-50 ml.

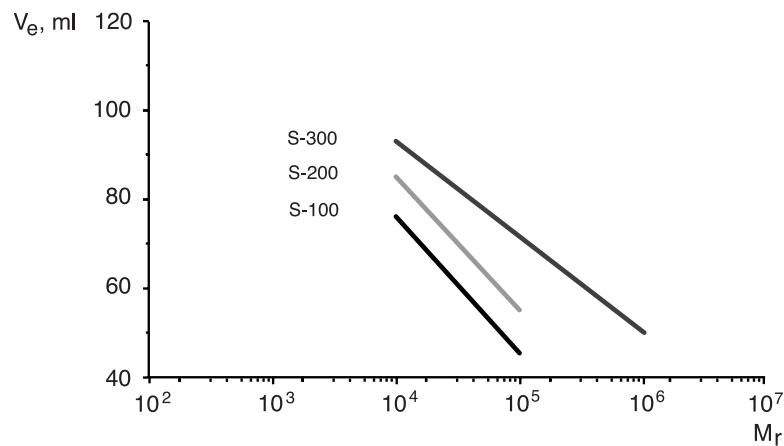


**Figure 9:** Selectivity curve for globular proteins on HiPrep 16/60 Sephacryl High Resolution columns.

For a standard run of SEC, the sample must be centrifuged initially at 4°C for 10 min at 16100 g to avoid loading precipitated protein in the system. Then, the sample is injected in a HiPrep 16/60 Sephacryl S-100 High-resolution (160 mL) column, pre-equilibrated in buffer C (300 mM NaCl, 40 mM Tris-HCl at pH 8). SEC is performed with a constant flow rate of 0.5 mL/min. The OYE detection is done the same way as for the AEX chromatography.

Finally, the protein is split into aliquots by using buffer C as diluent and with a final concentration of 10% glycerol. Aliquots are stored at -20°C.

### 4.3 Estimating purity with SDS-PAGE

A polyacrylamide gel electrophoresis (PAGE) in denaturing condition with the presence of sodium dodecyl sulfate (SDS) can give an approximate idea on how pure the solution is. First, the SDS, which is an anionic detergent, is used in order to linearize the proteins. It applies negatives charges elsewhere on the protein resulting in the straightening of the biomolecule because each charge repulses each other of the same sign. Once the SDS linearizes the proteins, they can be separated by their size through an acrylamide gel. It works like a grid containing several holes, depending on the percentage of acrylamide. The more holes there is, the slower bigger proteins will travel and the fastest the small one will migrate through the grid. An electric current going from the negative cathode toward the positive anode produces the flow. Since the proteins are negatively charged, they will be attracted toward the positive pole. A blue coomassie dye is added to samples in order to be able to follow the elution front. When it reaches the bottom of the gel, the migration is stopped. To see the results, the gel must be dyed. For this experiment, the gel is stained with a blue coomassie dye. An overall view of the migration and coloration is showed by the figure 10.

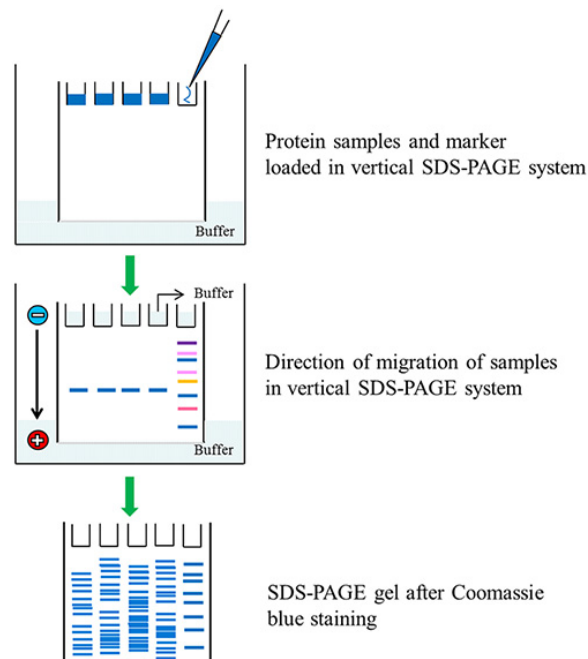


**Figure 10:** Overall schematic view of a SDS-PAGE analysis [34].

SDS-PAGE gel is prepared in order to get a final 10% acrylamide. Samples (cells after sonication, clear lysate, fraction after AEX and fraction after SEC) are mixed with deionized water and 4x SDS buffer before being denatured at 95°C for 10 minutes. After loading samples and the markers (Broad Range Ladder from BioRad), the gel is run at 200 V for 40 min. For the coloration, the gel is put in a box with the staining solution (1 g coomassie blue in 50% methanol) and warmed up in a microwaves oven for 30 s at max potency. After that, the gel is destained with a solution of 10% MeOH, 7% Glacial Acetic Acid in water. A piece of absorbing paper can be added in the box to trap the coomassie. Then, the box is slightly rocked for 5 min before removing the solution. Additional destaining steps may be required. When the gel is destained, it is stored digitally using a geldoc imager (Biorad). An OYE's band is visible corresponding to its molecular weight at 44 kDa.

#### 4.4 Determination of purified enzyme concentration

Protein concentration can be calculated by measuring the absorbance in the UV-vis region and applying equation 1:

$$A_x = \varepsilon_x \cdot [C] \cdot L \leftrightarrow [C] = \frac{A_x}{\varepsilon_x \cdot L}$$

**Equation 1:** Re-arranged Beer-Lambert law in order to be able to deduce concentration of a solution from its absorbance. Where  $A_x$  [-] is the absorbance at a wavelength of  $X$  [nm].  $\varepsilon_x$  is the molar extinction coefficient [ $\text{mM}^{-1} \cdot \text{cm}^{-1}$ ] at a wavelength of  $X$  [nm].  $[C]$  is the concentration of the solution [mM] and  $L$  is the length of the optical path [cm].

However, to use this formula, the molar extinction coefficient of each variant has to be experimentally determined. OYE1 has a FMN cofactor bound in its active site with a known extinction coefficient of the free form at 450 nm as  $11.3 \text{ mM}^{-1} \cdot \text{cm}^{-1}$ . By denaturing the enzyme, the flavin will be released and the absorbance of the free cofactor could be measured accurately. Assuming a ratio 1:1 (see equation 2), the concentration of the enzyme is equal to the concentration of FMN.



**Equation 2:** Stoichiometric equation between the OYE1 with and without its flavin cofactor.

The molar extinction coefficient of the enzyme is calculated using the equation 1.

Initially, the enzyme solution is centrifuged at 4°C for 10 min 16100 g. Supernatant is used for the measurement of the soluble OYE's spectrum from 300 to 800 nm. Secondly, the protein is denatured by adding 0.5% SDS final concentration and by boiling in the microwave 1 min at max potency. The solution is centrifuged at RT for 10 min 16100 g. The free flavin spectrum from is then measured. The max absorbances of the OYE1 (~450 nm) and of the free flavin (445 nm) are used for the calculation.

## 4.5 Enzymatic Assays

Because oxygen can be turned over by the enzyme consuming NADPH, the assays are done under anaerobic conditions in a hermetic chamber at room temperature with an orbital agitation. Within the reaction, the coenzyme NADPH is recycled by phosphite dehydrogenase, as shown in the following figure:

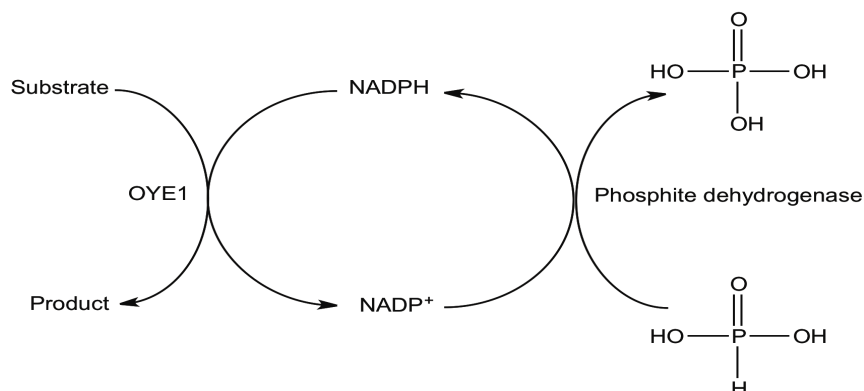


**Figure 11:** Representation of the enzymatic system applied during this work. The substrate is catalyzed by the OYE1 in the left half, while the cofactor is regenerated by the phosphite dehydrogenase in the right half.

For each measurement, 30  $\mu\text{L}$  of reaction were taken from the reaction vials at pre-determined time points. 50  $\mu\text{L}$  of ethyl acetate containing cyclohexanone (GC internal standard) are immediately added to quench the enzymatic reaction. The solution was well homogenized by shaking vigorously for 1 minute. To enhance phase separation, the tubes were centrifuged at RT for 2.5 min and 16100 g. Finally, the organic phase was analyzed by GC with the corresponding method. Table 5 shows the concentration of each constituent in the reaction vial per substrate.

**Table 5:** Composition of enzymatic reactions according to the substrate used. NaPi stands for sodium phosphate.  $\text{NADP}^+$  for Nicotinamide adenine dinucleotide phosphate and PTDH for phosphite dehydrogenase. S/R-1 are for S/R-carvone. 3 is for trans  $\alpha$ -methylcinnamaldehyde. 5 is for myrtenol. 7 stand for methyl 2-hydroxymethylacrylate. 9 is for 4-phenyl-3-buten-2-one and (E/Z)-12 is for E/Z-citral.

	(S)-1	(R)-1	3	5	7	9	(E/Z)-12
[Substrate]	200 $\mu\text{M}$	200 $\mu\text{M}$	2 mM	500 $\mu\text{M}$	600 $\mu\text{M}$	200 $\mu\text{M}$	600 $\mu\text{M}$
[Enzyme]	1 $\mu\text{M}$						
[NaPi]	10 mM						
[FMN]	5 $\mu\text{M}$						
[ $\text{NADP}^+$ ]	100 $\mu\text{M}$						
[PTDH]	1 $\mu\text{M}$						
[Cyclohexanone]	500 $\mu\text{M}$	500 $\mu\text{M}$	1 mM	500 $\mu\text{M}$	500 $\mu\text{M}$	500 $\mu\text{M}$	500 $\mu\text{M}$

### 4.5.1 Calculations of relative concentrations

Results shown as relative concentrations are calculated according equation 3.

$$\frac{C_x}{(C_x + C_y + \dots + C_n)} \cdot 100 = \text{Relative concentration of } C_x \text{ [\%]}$$

**Equation 3:** Calculation of relative concentration of a compound X in a reaction with N components.

### 4.5.2 Calculation of enantiomeric excess

Enantiomeric excess (*ee*) are calculated according equation 4.

$$\frac{A - B}{A + B} \cdot 100 = ee_A$$

**Equation 4:** Calculation of the enantiomeric excess for A, which is the predominant specie among products.

### 4.5.3 Calculation of conversion rates

Conversion rates are determined from quantitative data (figures in appendix 10.4.1 to 10.4.6) by using the slope of the linear regression of the consumption of substrate. Regressions are done with GraphPad Prism 6.

$$\frac{\text{slope} \left[ \frac{\mu\text{M}_{\text{substrate}}}{\text{min}} \right]}{n_{\text{enzyme}} [\text{nmol}_{\text{enzyme}}]} = \text{Conversion rate} \left[ \frac{\mu\text{M}_s}{\text{min} \cdot \text{nmol}_E} \right]$$

**Equation 5:** Calculation of conversion rate from the slope of a linear regression of quantitative data of components against time.

## 4.6 Gas Chromatography analysis

Enantioselectivity and catalytic activity were determined following the consumption of starting material and the appearance of product by gas chromatography (GC) analysis. This instrument allows the separation of components through a capillary column. The mobile phase is a gas (i.e. hydrogen) and the compounds are vaporized in the injector so they also enter the system in gas phase. Then, the sample arrives in the column, which is installed in an oven. The instrument is programmable allowing the creation of defined methods that control the temperature of the system. The operator can choose between various modes: isothermal (same temperature over a selected duration of time), gradient (temperature increase with a chosen slope) or even a mix of both modes.

The column used in this work (Cyclosil B, Agilent, 30 m long, 0.25  $\mu\text{m}$  film thickness) is coated with 30% heptakis (2,3-di-O-methyl-6-O-t-butyl-dimethylsilyl)- $\beta$ -cyclodextrin (figure 12), which is a functionalized cyclodextrin.

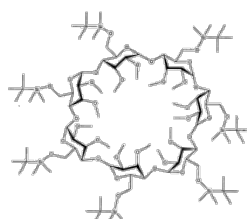


**Figure 12:** Scheme of a Heptakis(2,3-di-O-methyl-6-O-t-butyl-dimethylsilyl)- $\beta$ -cyclodextrin, which is a functionalized cyclodextrin found on a Cyclosil-B (Agilent) stationary phase.

The principle is very similar to the SEC. Cyclodextrins can be imagined like barrels, which allows compounds (usually, the desired analyte) to get in it to form a complex, before being released (figure 13). This interaction depends on several factors. There are the hydrophobic interactions, the van der Waals attractions, any hydrogen bonding or electrostatic interactions that can retain a molecule guest inside a cyclodextrin. The molecules that enter the cyclodextrins will travel longer through the column than the ones that do not get inside the barrels. The difference of speed obtained between compounds will result in a separation of the components throughout the column.

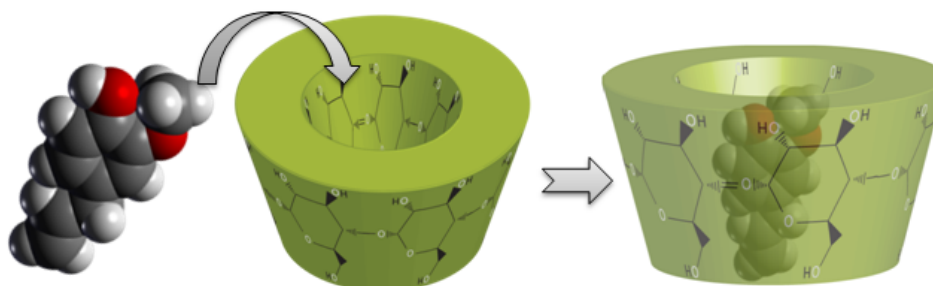


**Figure 13:** Non-functionalized Cyclodextrin (green barrel) capturing a molecule.

At the end of the column, there is a flame ionization detector (FID). As its name suggest, the detector uses a flame to ionize analyte molecules coming out of the column. The ions formed then interact with the electrodes of the detector to generate electrical signals. This process is depicted in figure 14.

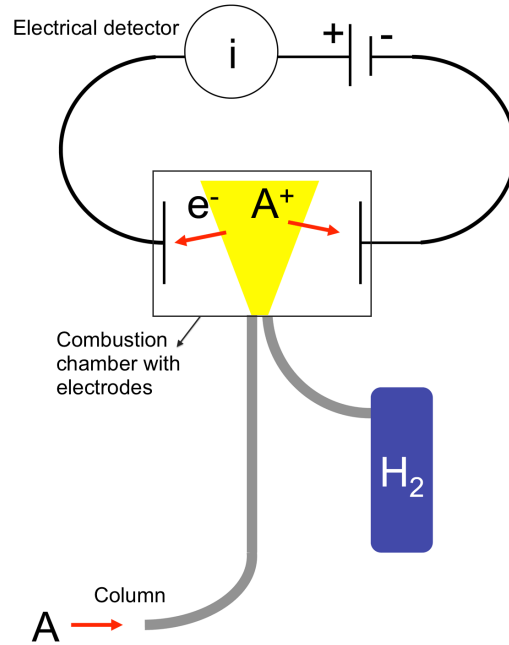


**Figure 14:** Flame ionization detector scheme. « A » stands for Analyte. Once it is burnt, it releases an electron ( $e^-$ ) and thus, become positively charged ( $A^+$ ), those ions are detected by the electrodes in the combustion chamber. Then, the electrical detector gives a signal corresponding to the excitation of the electrodes.

In every sample, an internal standard was added. It is a molecule that does not interact with any other component in the injected solution and that is present at the same concentration. The utility of this standard is to reduce the impact of the error created by the injector, which does not always inject the exact same volume in the column. Since the concentration of internal standard is identical in every sample, injector inconsistencies can be overcome by normalizing analyte peak areas relative to the internal standard peak areas. Once this is done, areas from separate injections can be confidently compared between each other.

#### 4.6.1 (S/R)-carvone

The method is the following: Start at 90°C and hold 5 min. Then increase temperature 1°C/min until 120°C and hold for 15 min, total run time of 35 min. Injector and detector are set at 250 and 250°C respectively. The H<sub>2</sub> flow is set constant at 1.8 ml/min with a front pressure of 36.6 kPa. 1  $\mu$ L is injected with a split of 1:1. Retention times for (S/R)-carvone are 27.5 and 27.6 min respectively. (2S,5S)- (2R,5S)-carvone have retention times of 22.9 and 23.1 min, while retention time for (2R,5R)-carvone is 22.7 min.

#### 4.6.2 *Trans* $\alpha$ -methyl-cinnamaldehyde

The method is the following: Isothermal, 150°C hold 10 min. Injector and detector are set at 250 and 200°C respectively. The H<sub>2</sub> flow is set constant at 1.8 ml/min with a front pressure of 45.7 kPa. 1  $\mu$ L is injected with a split of 25.1:1. The retention time for *trans*  $\alpha$ -methyl-cinnamaldehyde is 6.3 min. S-cinnamaldehyde has a retention time of 3.8 min.

#### 4.6.3 Myrtenol

The method is the following: Start at 90°C and hold for 1 min. Then increase temperature 3°C/min until 120°C and hold 19 min, total run time 20 minutes. Injector and detector are set at 250 and 310°C respectively. The H<sub>2</sub> flow is set constant at 4 ml/min with a front pressure of 71.2 kPa. 1  $\mu$ L is injected with a split of 1:1. Retention time for myrtenol is 11.7 min. (+)-*trans*-myrtenol has a retention time of 16.1 min.

#### 4.6.4 Methyl 2-hydroxymethylacrylate

The method is the following: Starting at 60°C and hold 1 min. Then, 1°C/min until 75°C, hold 4 min, total run time 20 minutes. Injector and detector are set at 280 and 200°C respectively. The H<sub>2</sub> flow is set constant at 4 ml/min with a front pressure of 68.6 kPa. 1  $\mu$ L is injected with a split of 1:1. Retention times for *trans* methyl 2-hydroxymethylacrylate is 16.8 min. Methyl (R)-(-)- $\beta$ -hydroxyisobutyrate and methyl (S)-(+)-3-hydroxy-2-methylpropionate have retention times of 15.2 and 17.0 min.

#### 4.6.5 4-phenyl-3-butyne-2-one

The method is the following: Start at 70°C and hold 1 min. Then, increase temperature 2°C/min until 110°C and hold 15 min, total run time 36 minutes. Injector and detector are set at 250 and 310°C respectively. The H<sub>2</sub> flow is set constant at 4 ml/min with a front pressure of 71 kPa. 1  $\mu$ L is injected with a split of 1:1. Retention time for 4-phenyl-3-butyne-2-one is 23.4 min. For the 4-phenyl-3-buten-2-one and the 4-phenyl-2-butanone, retention times are 34.6 and 21.9 min.

#### 4.6.6 (E/Z)-citral

The method is the following: Start at 80°C, increase temperature 2.5°C/min until 115°C and hold 2 min, total run time 16 minutes. Injector and detector are both set at 270°C. The H<sub>2</sub> flow is set constant at 4 ml/min with a front pressure of 68.5 kPa. 1  $\mu$ L is injected with a split of 1:1. E/Z-citral peaks could not be identified because enantiopure solutions are not commercially available. However, the separation was possible and the E/Z-mixture gave two peaks, which retention times are 13.1 and 14.9 min. (S/R)-citronellal retention time are 9.057 min and 9.018 min respectively.

## 5. Results

### 5.1 Enzyme purification

Following expression the harvested cells (6.4 g) were lysed for a final 40 mL of clarified lysate. The sample was loaded on the Anion Exchange and purification proceeded as described into the materials and methods. Fractions were collected between 80 and 100 mL corresponding to the elution of the flavin peak at 460nm. An AEX chromatogram is showed in the figure 40 in the appendix 10.2.

Harvested fractions were concentrated down and then injected on the SEC. OYE1 elute between 46 and 55 mL corresponding to a MW of about 88 kDa as OYE1 is a dimer in solution (SEC chromatogram showed in figure 41 appendix 10.3).

Collected protein fractions were loaded on a 10% acrylamide SDS-page gel and migrated for 40 min at 200 V. OYE's band is visible at ~44 kDa, consistent with its reported molecular weight.

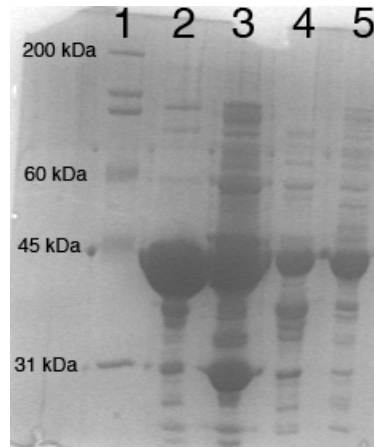


**Figure 15:** 10% acrylamide SDS-page gel migrated for 40 min at 200 V and stained with coomassie blue. 1) Broad Range Ladder from BioRad, 2) Wild Type OYE, 3) cp303OYE, 4) W116IOYE, 5) cp303OYEW116I.

### 5.2 Calculation of enzyme concentration

The molar extinction coefficients of W116I and cp303W116I variants were determined with spectrophotometric assays as described in the materials and methods.

**Table 6:** Values obtained and used during the experiment for the determination of the molar extinction coefficient of W116I and cp303W116I enzymes. Calculations are based on the equation 1.

	<b>W116I</b>	<b>cp303W116I</b>
OYE1 $A_{\max}$	0.116	0.056
Free FMN $A_{445}$	0.0651	0.0522
$\epsilon_{\text{FMN}}$ [ $\text{mM}^{-1}\text{cm}^{-1}$ ]	12.5	12.5
Dil. Factor	2	1
FMN=OYE1 [mM]	0.0104	0.0042
$\epsilon_{\text{OYE}}$ [ $\text{mM}^{-1}\text{cm}^{-1}$ ]	11.1	13.4

### 5.3 Catalytic rate and enantioselectivity of mutants

Relative concentrations values used for figures 16, 17, 20, 26, 29 and 35 as well as quantitative data are shown in appendix 10.4.1 to 10.4.6.

#### 5.3.1 (*S*)-carvone

Both the enzymatic assay and GC method have been previously optimized [1]. The initial concentration of 200  $\mu$ M of substrate was chosen to ensure the most representative conversion in 3 hours. Retention times were obtained from reference molecules. Quantitative data were calculated from a standard curve. However the enantiomerically pure products of the reaction are not commercially available, quantitative data of the products is calculated using (*S*)-carvone calibration curve (which could cause not accurate measures). Figure 16 shows evolution of relative concentrations over time.

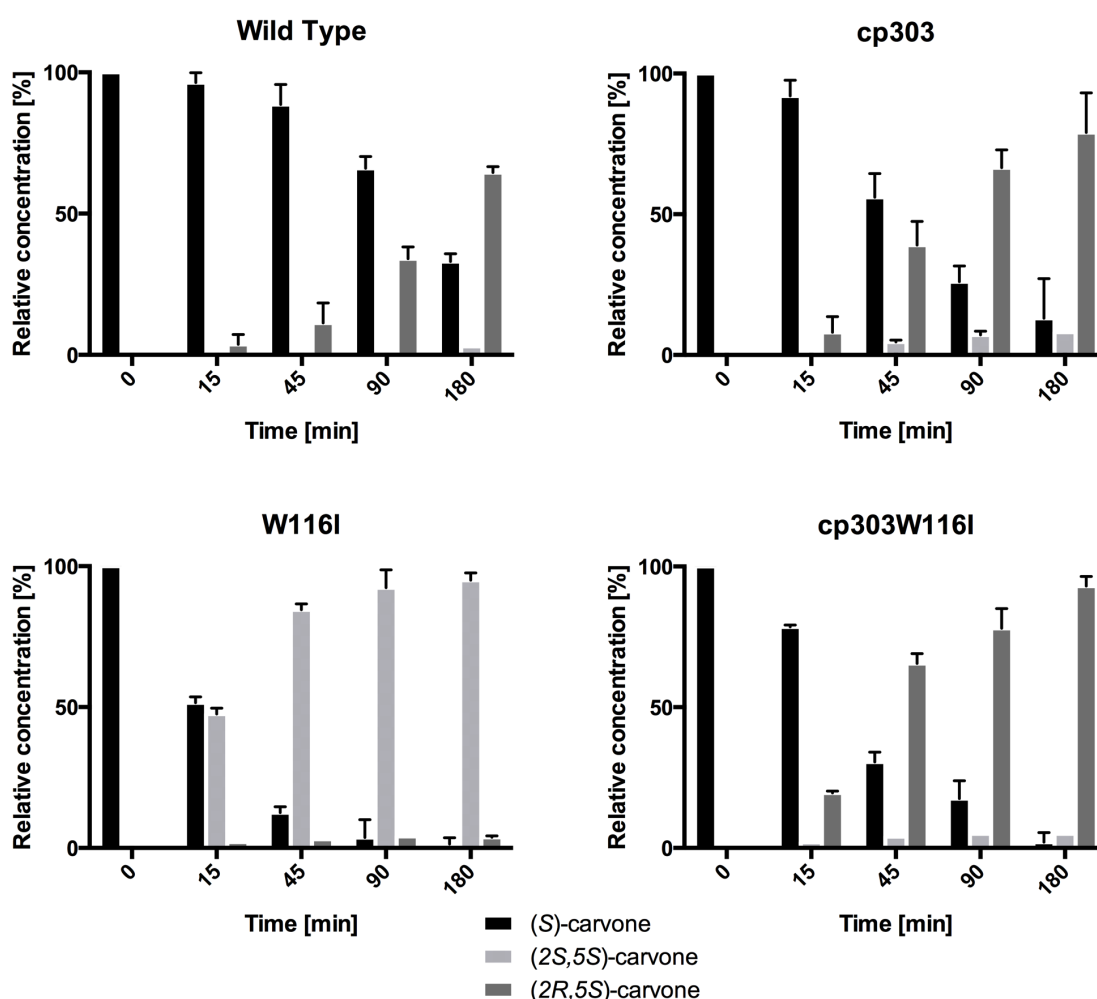


**Figure 16:** Conversion of (*S*)-carvone into (*2S,5S*)- or (*2R,5S*)-carvone by WT and its variants. Experiments are done in buffer A (20 mM NaCl, 40 mM Tris-HCl, pH 8 at 20°C) with 200  $\mu$ M of (*S*)-I as starting material using phosphite dehydrogenase and NaPi as cofactor regenerating system.

Table 7 shows the calculated enantiomeric excess (*ee*) and conversion rates for (**S**)-1.

**Table 7:** Enantiomeric excess (*ee*) in percent and conversion rate expressed as  $\left[\frac{\mu\text{M}_S}{\text{min}\cdot\text{nmol}_E}\right]$  for each variant with (**S**)-carvone as substrate.

Enzyme	<i>ee</i>	Conversion Rate
Wild Type	91 ( <i>R</i> )	3.8 ± 0.3
cp303	79 ( <i>R</i> )	7.5 ± 0.4
W116I	91 ( <i>S</i> )	17.6 ± 2.6
cp303W116I	88 ( <i>R</i> )	13.8 ± 1.1

### 5.3.2 (*R*)-carvone

Due to the similarities with the other enantiomer, (**R**)-1, experiments were done with 200  $\mu\text{M}$  starting material, 1  $\mu\text{M}$  enzyme and the same time points. As mentioned before, the enantiomerically pure products (*2R,5R*)- and (*2S,5R*)-carvone are not commercially available. Therefore, quantitative data of the products is calculated from (*R*)-carvone calibration curve (which could cause not accurate measures). Figure 17 shows evolution of relative concentrations over time.

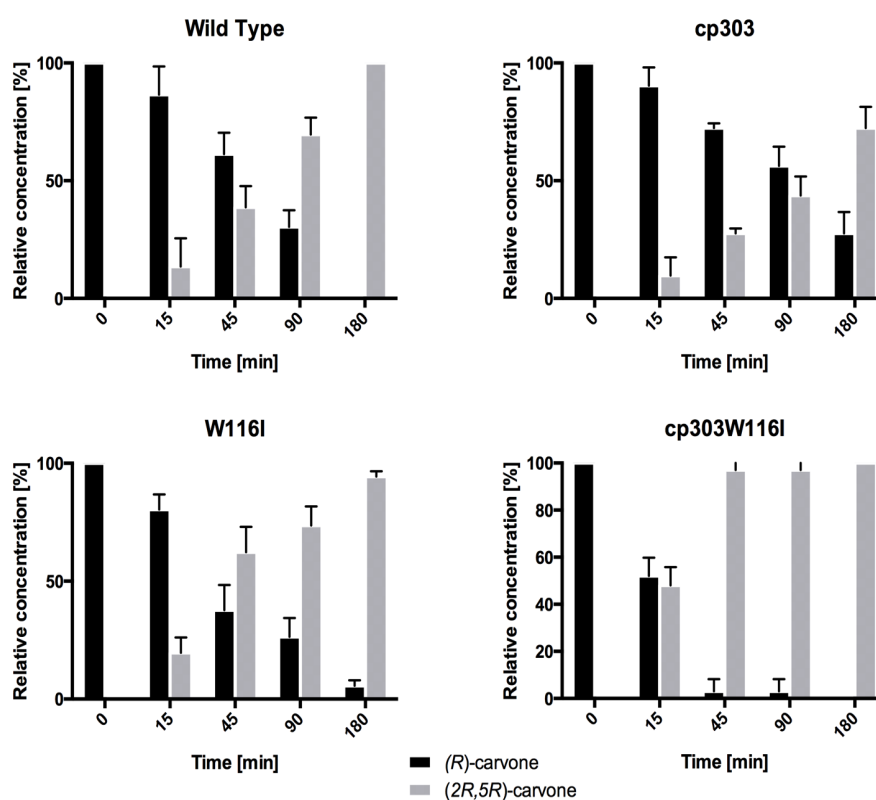


**Figure 17:** Conversion of (*R*)-carvone into (*2R,5R*)-carvone by WT and its variants. Experiments are done in buffer A (20 mM NaCl, 40 mM Tris-HCl, pH 8 at 20°C) with 200  $\mu\text{M}$  of (**R**)-1 as starting material using phosphite dehydrogenase and NaPi as cofactor regenerating system.

Table 8 shows the enantiomeric excess (*ee*) and conversion rates for (*R*)-1.

**Table 8:** Enantiomeric excess (*ee*) in percent and conversion rate expressed as  $\left[\frac{\mu\text{M}_s}{\text{min}\cdot\text{nmol}_E}\right]$  for each variant with (*R*)-carvone as substrate.

Enzyme	<i>ee</i>	Conversion Rate
Wild Type	> 99 ( <i>R</i> )	4.3 ± 0.3
cp303	> 99 ( <i>R</i> )	2.2 ± 0.2
W116I	> 99 ( <i>R</i> )	7.0 ± 0.4
cp303W116I	> 99 ( <i>R</i> )	9.1 ± 0.8

### 5.3.3 *Trans* $\alpha$ -methyl-cinnamaldehyde

The GC method for this molecule was already designed. However, a few adjustments were necessary since the last molecule was eluted after 6 min. Thus, the method was shortened to a total run time of 10 min without affecting the quality of separation. Several concentrations of starting material were investigated in order to get a significant consumption over time.

Concentrations between 200  $\mu\text{M}$  and 10 mM were tested (200, 500  $\mu\text{M}$  and 2, 3, 5, 10 mM). With **3** under 2 mM, the starting material was consumed too fast to accurately collect data points. At higher concentrations, the rates of conversion slowed down suggesting a possible substrate inhibition. Considering the 8% yield for the extraction in ethyl acetate, a compromise had to be found in order to have a sufficient area (30-200 pA\*s) during the GC analysis and enough substrate to let time to get accurate time points.

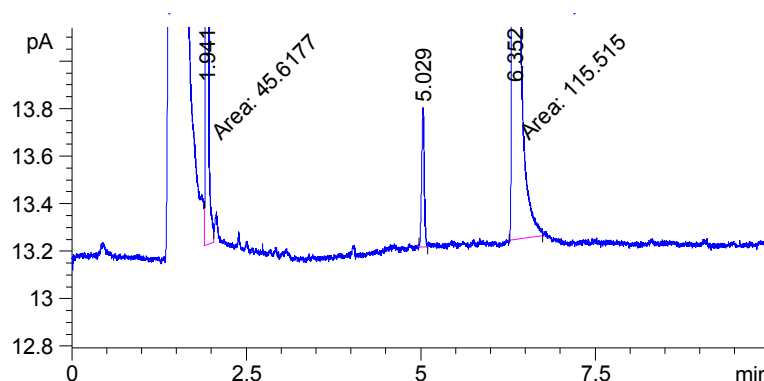


**Figure 18:** Time point after 90 min of an enzymatic assay using 10 mM *trans*  $\alpha$ -methyl-cinnamaldehyde as substrate and 1  $\mu\text{M}$  Wild Type OYE1 as enzyme. The temperature program is 150°C isothermal for 10 min on a Cyclosil-B column from Agilent. Retention times are: 1.9 min for cyclohexanone (internal standard), 5 min for (*S*)-cinnamaldehyde and 6.3 min for the starting material. The area of the product is 1.52 pA\*s.

At 2 mM it was possible to observe a 50% conversion after 45 min. Time points were then adjusted to 0/10/20/45/90 min in order to obtain the most comprehensive data over time.

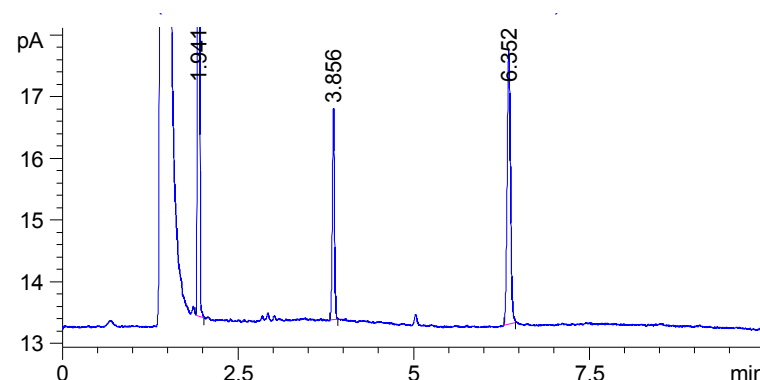


**Figure 19:** Time point after 45 min of an enzymatic assay using 2 mM *trans*  $\alpha$ -methyl-cinnamaldehyde and 1  $\mu$ M Wild Type OYE1. The temperature program is 150°C isothermal for 10 min on a Cyclosil-B column from Agilent. Retention times are: 1.9 min for cyclohexanone (internal standard), 3.8 min for (*S*)-cinnamaldehyde and 6.3 min for the starting material. The areas for the cyclohexanone, the product and the starting material are 44.78, 7.17 and 14.89 pA\*s respectively.

Quantitative data is calculated from a standard curve. As before, the products of the reaction cannot be purchased, quantitative data of the products is calculated from 3-phenylpropionaldehyde calibration curve. This may cause a non-accurate determination of the concentrations of the product. The product was defined as (*S*)-4 because literature [35] was reporting this molecule as only product. Figure 20 shows evolution of relative concentrations over time.

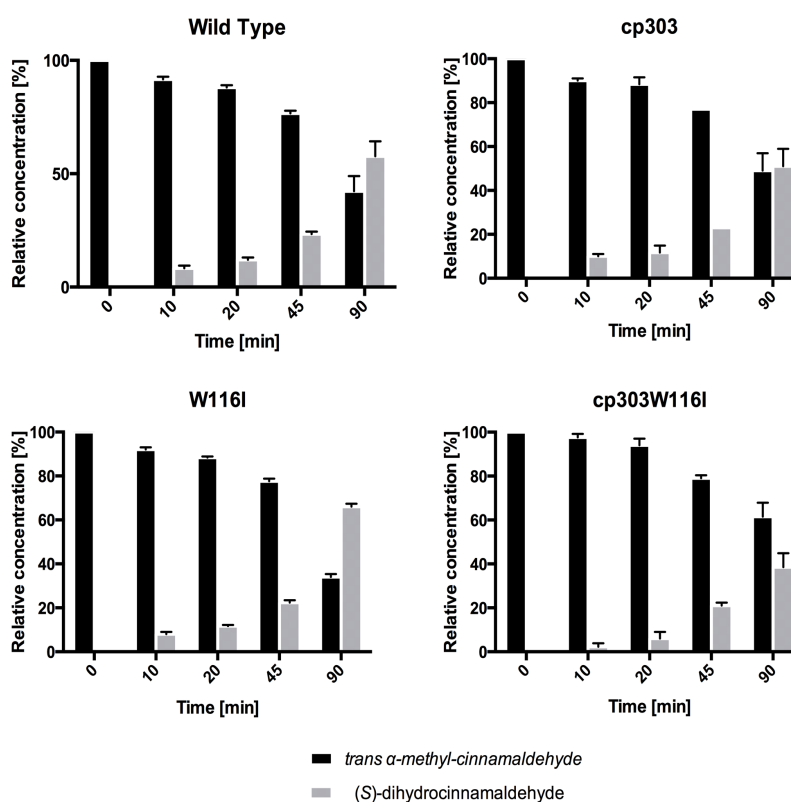


**Figure 20:** Conversion of *trans*  $\alpha$ -methyl-cinnamaldehyde into (*S*)-dihydrocinnamaldehyde by Wild Type OYE1 and its variants. Experiments are done in buffer A (20 mM NaCl, 40 mM Tris-HCl, pH 8 at 20°C) with 2 mM of 3 as starting material using phosphite dehydrogenase and NaPi as cofactor regenerating system.

Table 9 shows enantiomeric excess (*ee*) and conversion rates for *trans*  $\alpha$ -methyl-cinnamaldehyde.

**Table 9:** Enantiomeric excess (*ee*) in percent and conversion rate expressed as  $\left[\frac{\mu\text{M}_S}{\text{min}\cdot\text{nmol}_E}\right]$  for each variant with *trans*  $\alpha$ -methyl-cinnamaldehyde as substrate.

Enzyme	<i>ee</i>	Conversion Rate
Wild Type	>99 ( <i>S</i> )	78 $\pm$ 5.9
cp303	>99 ( <i>S</i> )	70.3 $\pm$ 3.9
W116I	>99 ( <i>S</i> )	68.9 $\pm$ 3.4
cp303W116I	>99 ( <i>S</i> )	47.7 $\pm$ 4.6

### 5.3.4 Myrtenol

Initially, the method was set with an isothermal temperature at 150°C for 45 min. The result gave a myrtenol peak eluting within the tail of the solvent peak (figure 21).

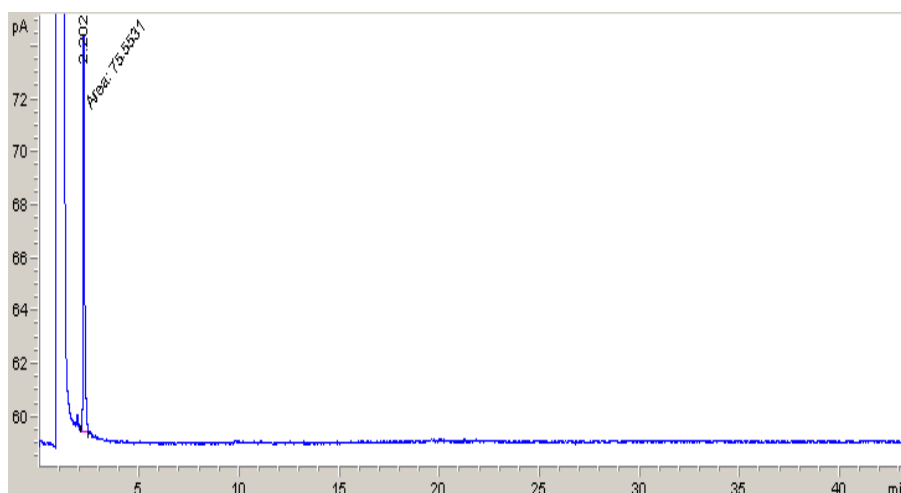


**Figure 21:** Injection of 1  $\mu\text{L}$  from a 200  $\mu\text{M}$  myrtenol solution. The temperature program was 150°C hold for 45 min on a Cyclosil-B column from Agilent. myrtenol peak is at 2.2 min.

In order to increase the retention time, the temperature was lowered. Several temperatures were investigated, 90°C gave the best results. A slope of 3°C/min from 90 to 120°C was added in order to fasten the overall retentions times and peak shape.

As shown by figure 22, **5** was eluted at 11.7 min, away from the solvent, the internal standard, and the product.

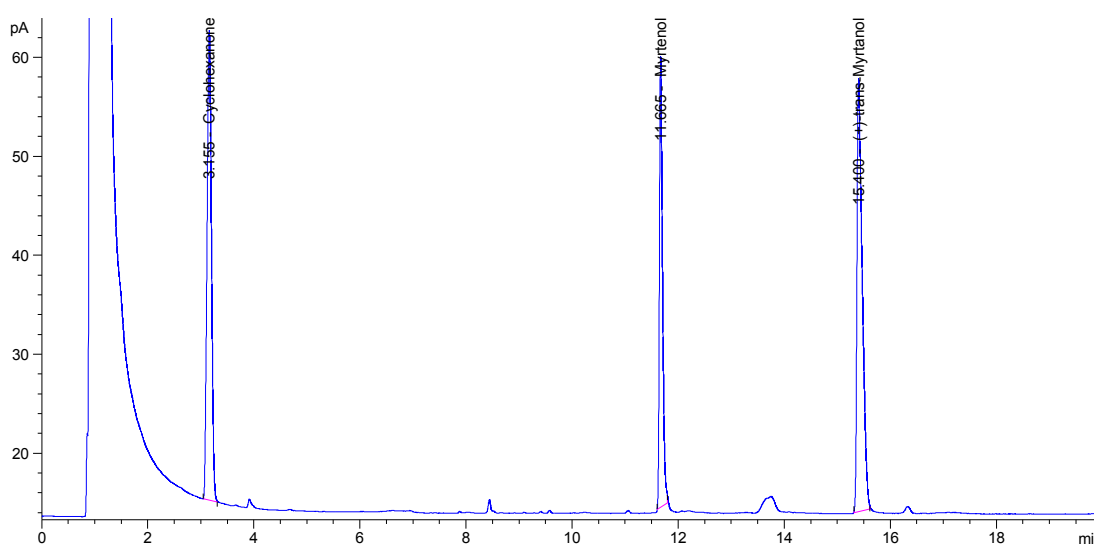


**Figure 22:** Injection of 1  $\mu\text{L}$  from a 200  $\mu\text{M}$  myrtenol, 200  $\mu\text{M}$  (+)-trans-myrtanol solution containing 500  $\mu\text{M}$  cyclohexanone. The temperature program was 90°C hold 1 min, then 3°C/min until 120°C, hold 19 min on a Cyclosil-B column from Agilent. Cyclohexanone peak is at 3.1 min, myrtenol peak is at 11.6 min and (+)-trans-myrtanol peak is at 15.4 min.

All samples were directly diluted in ethyl acetate during the method optimization. Once the GC program was set, the extraction from buffer A was investigated. Usually, molecules were well extracted from the buffer. However, this was not the case with myrtenol and especially the (+)-trans-myrtanol: their extractions yielded 19.3 and 7.2 % respectively. Several alternatives were investigated.

When selecting another extraction solvent, polar solvents could not be used (would be miscible with water). Therefore, n-hexanes were chosen because of its non-polar character. This solvent gave a 16.7 % yield for the extraction of myrtenol from buffer A. This value was lower than with the ethyl acetate, (+)-trans-myrtanol was not investigated with this solvent. Secondly, the substrate concentration was increased to 1 mM, so the low yield of extraction would be compensated with the high concentration. An assay was run with 1  $\mu\text{M}$  WT, 1 mM of myrtanol and the habitual concentration of the other components (see table 5). After 3 hours of reaction, the starting material was still not consumed. The same assay was ran but with 5  $\mu\text{M}$  of enzyme in order to avoid a possible substrate inhibition. This last assay showed the same tendency as the previous one, no myrtenol consumption after 3 hours. Two other assays were done at 500 and 200  $\mu\text{M}$  with 1  $\mu\text{M}$  WT and habitual concentration of the other components (table 5). No consumption was recorded, neither after 24 h reaction. Enzymatic assays were done with 500  $\mu\text{M}$  myrtenol for the other enzymes (cp303OYE, W116IOYE and cp303OYEW116I). This concentration was chosen in order to avoid any possible substrate inhibition. It resulted in a non-consumption of the substrate after a 3 hours reaction.

### 5.3.5 Methyl 2-hydroxymethylacrylate

Initially, a standard method with a long run (over 30 min) has been used to evaluate the retention time of the molecule. The results showed that the methyl 2-hydroxymethylacrylate was coming off the column very early (figure 23) and that the (*R*)-Roche Ester (reduced form) had a very similar retention time. Temperatures had to be lowered in order to increase their retention times and improve their resolution.

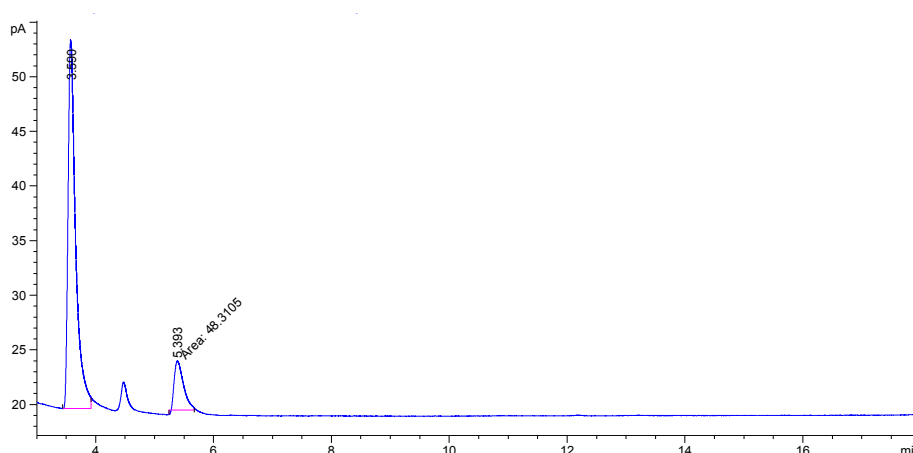


**Figure 23:** Injection of 1  $\mu\text{L}$  from a 200  $\mu\text{M}$  methyl 2-hydroxymethylacrylate solution containing 500  $\mu\text{M}$  cyclohexanone. The temperature program is 90°C hold for 1 min, then 1°C/min until 120°C hold 19 min on a Cyclosil-B column from Agilent. Cyclohexanone peak is at 3.59 min, while methyl 2-hydroxymethylacrylate peak is at 5.39 min. The small peak between them is a contamination from the solvent (ethyl acetate).

An on going problem with the chromatograms was that the peaks were too wide and had significant tailing. This was resulting in a low resolution between components with close retention times. In order to improve the shape of the peaks, their resolution and their retention times, lower starting temperatures were investigated (90, 75, 60°C). As shown by figure 24, it was possible to obtain good separation between peaks with the 60°C method.

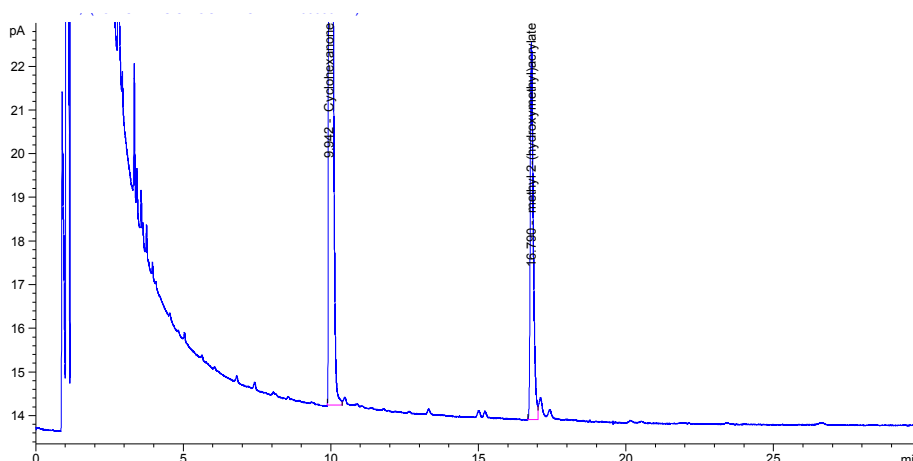


**Figure 24:** Injection of 1  $\mu\text{L}$  from a 200  $\mu\text{M}$  methyl 2-hydroxymethylacrylate solution containing 500  $\mu\text{M}$  cyclohexanone. 60°C hold 1 min, then 1°C/min to 75°C, hold 14 min on a Cyclosil-B column from Agilent.

Finally, the method was shortened to a 20 min total time without affecting the quality of the separation in the following run (see figure 25). All compounds were identified and quantified with the help of reference molecules bought from Acros Organics.

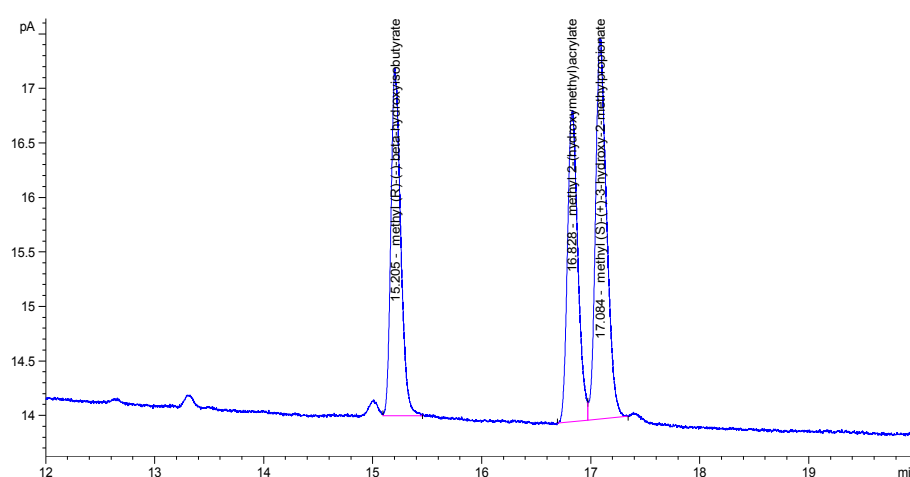


**Figure 25:** Injection of 1  $\mu\text{L}$  from a 70  $\mu\text{M}$  methyl 2-hydroxymethylacrylate, 70  $\mu\text{M}$  Methyl (R)-(-)- $\beta$ -hydroxyisobutyrate and 70  $\mu\text{M}$  Methyl (S)-(+)-3-hydroxy-2-methylpropionate solution containing 500  $\mu\text{M}$  cyclohexanone. 60°C hold 1 min, then 1°C/min to 75°C, hold 14 min on a Cyclosil-B column from Agilent.

The last parameter to evaluate was the extraction efficiency. 200  $\mu\text{M}$  of **7** and (**S/R**)-**8** were extracted from buffer A with ethyl acetate. It yielded to an efficiency of 40%. In order to overcome the extraction factor on the area obtained throughout the GC analysis, the starting concentration of **7** was increased to 600  $\mu\text{M}$ . It will be the minimum concentration usable to be able to get consistent GC data.

An enzymatic assay with 1  $\mu\text{M}$  of WT showed that the conversion of the substrate over time is very slow. A small proportion of total starting molecule was consumed after 180 min. In order to confirm this assumption, the same assay was done with 5  $\mu\text{M}$  enzyme instead. Results were consistent and still showed a slow reaction (figure 26). Because of time issues, this substrate was not investigated with other variants. Figure 26 shows evolution of relative concentrations over time.

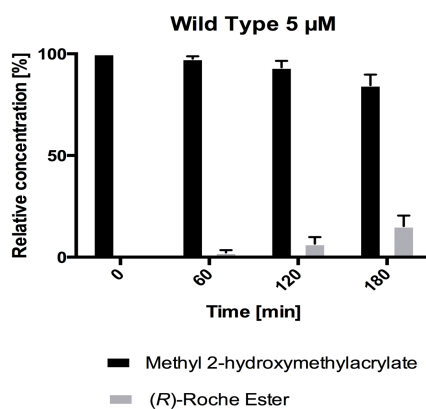


**Figure 26:** Conversion of methyl 2-hydroxymethylacrylate into (R)-Roche Ester by WT and its variants. Experiment is done in buffer A (20 mM NaCl, 40 mM Tris-HCl, pH 8 at 20°C) with 600  $\mu\text{M}$  of **7** as starting material using phosphite dehydrogenase and NaPi as cofactor regenerating system.

Table 10 shows enantiomeric excess (*ee*) and conversion rate for **7**.

**Table 10:** Enantiomeric excess (*ee*) in percent and conversion rate expressed as  $\left[\frac{\mu\text{M}_S}{\text{min}\cdot\text{nmol}_E}\right]$  for wild type OYE1 with methyl 2-hydroxymethylacrylate as substrate.

Enzyme	<i>ee</i>	Conversion Rate
Wild Type	> 99% ( <i>R</i> )	0.8 ± 0.1

### 5.3.6 4-phenyl-3-butyn-2-one

The first program tried was adapted from the (**S**)-**1** method because no reference about **9** being separated with a Cyclosil-B column was found in the literature and that (**S**)-**1** method was the only known method. Before starting, a few modifications were done: the initial oven temperature was lowered to 70°C instead of 90°C, as well as the final temperature that was lowered to 110°C instead of 120°C. A lower temperature was set up in order to allow the molecule to stay longer in the column and avoid a possible early elution. In order to improve the sensitivity, the detector temperature was increased to 310°C, therefore a maximum amount of molecule will be detected at the end of the column. The flow rate was not changed and stayed constant at 2 mL/min (46 cm/s).

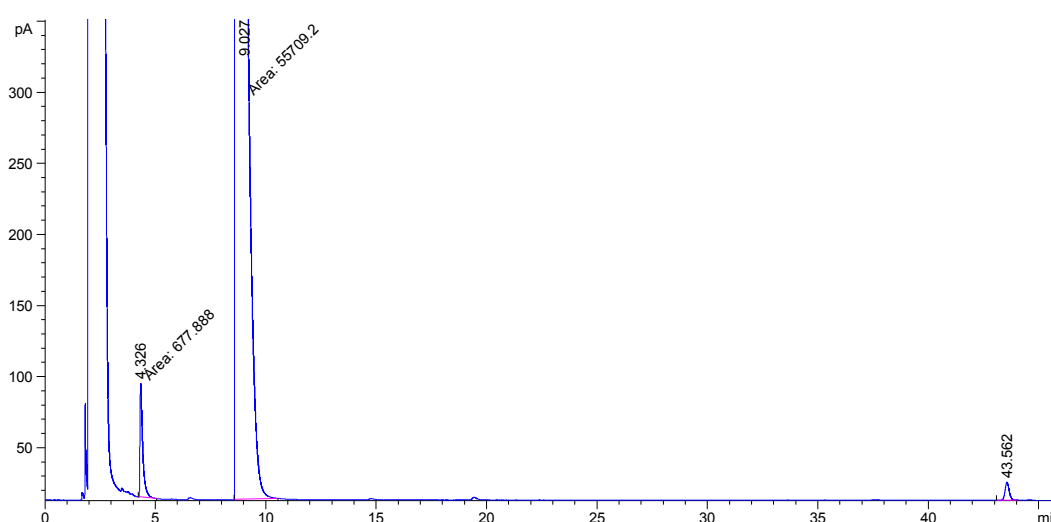


**Figure 27:** Injection of 1  $\mu\text{L}$  from a 200  $\mu\text{M}$  4-phenyl-3-butyn-2-one solution. The temperature program is 70°C hold for 1 min, then 1°C/min to 110°C and hold 5 min on a Cyclosil-B column from Agilent. Peak at 4.3 min is the 1 mM of cyclohexanone, peak at 9.0 min is the DMSO solvent used for the pre-dilution of **9**, peak at 43.5 min is the 4-phenyl-3-butyn-2-one, its area is 157.01 pA\*s.

DMSO was used during a pre-dilution for this run for solubility tests purpose. Following experiments were done without dimethyl sulfoxide without affecting the quality of the separation.

Separation of **9** in the figure 27 is already acceptable. However, the retention time is long. In order to reduce it, the flow was increased to constant rate of 4 mL/min (71 cm/s) and the temperature slope was increased from 1 to 2°C/min. The internal standard concentration was adjusted in order to inject an amount between 20 and 50 ng to avoid a column overload.

The results of the previous modifications are shown in figure 28.

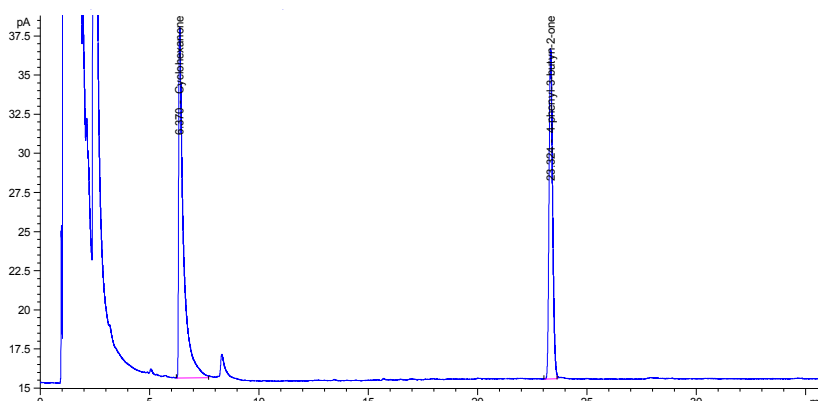


**Figure 28:** Injection of 1  $\mu$ L from a 200  $\mu$ M 4-phenyl-3-butyn-2-one solution. The temperature program is 70°C hold for 1 min, then 2°C/min to 110°C and hold 5 min on a Cyclosil-B column from Agilent.

An assay with 200  $\mu$ M **9** and 1  $\mu$ M WT OYE1 gave a full conversion after 180 min. Time points were then adjusted to 0/15/45/90/180 min in order to have the most understandable vision of the substrate consumption. All compounds were identified and quantified with the help of reference molecules bought from Acros Organics. Figure 29 shows evolution of relative concentrations over time.

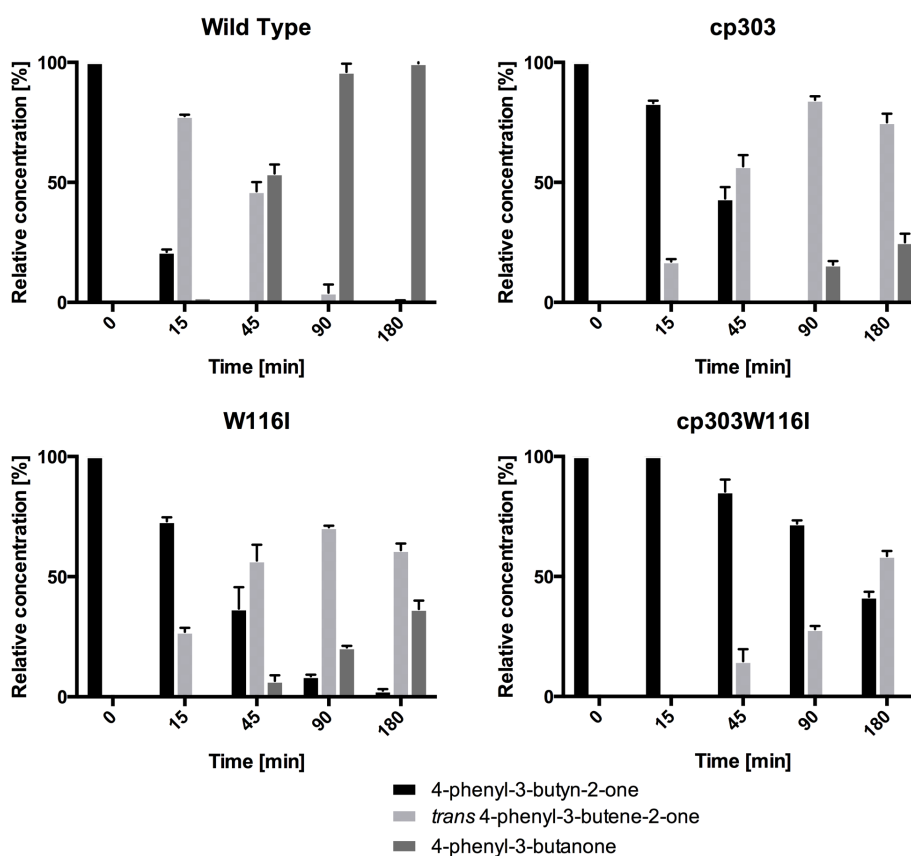


**Figure 29:** Conversion of 4-phenyl-3-butyn-2-one into *trans* 4-phenyl-3-butene-2-one and 4-phenyl-3-butanone by WT and its variants. Experiments are done in buffer A (20 mM NaCl, 40 mM Tris-HCl, pH 8 at 20°C) with 200  $\mu$ M of **9** as starting material using phosphite dehydrogenase and NaPi as cofactor regenerating system

Table 11 shows enantiomeric excess (*ee*) as well as the conversion rates for **9**.

**Table 11:** Enantiomeric excess (*ee*) in percent and conversion rate expressed as  $\left[\frac{\mu\text{M}_S}{\text{min}\cdot\text{mmol}_E}\right]$  for each variant with 4-phenyl-3-butyn-2-one as substrate.

Enzyme	<b>9 to E/Z-10</b>		<b>E/Z-10 to 11</b>	
	<i>ee</i>	Conversion Rate	<i>ee</i>	Conversion Rate
Wild Type	>99 (Z)	50.7 ± 9.7	-	21.7 ± 2.3
cp303	>99 (Z)	22.9 ± 1.7	-	0.4 ± 0.1
W116I	>99 (Z)	37.7 ± 3.9	-	0.9 ± 0.1
cp303W116I	>99 (Z)	3.5 ± 0.3	-	0.4 ± 0.04

### 5.3.7 (E/Z)-Citral

The first method that was used for (E/Z)-**12** did not give a proper separation, as it is possible to see in figure 30.

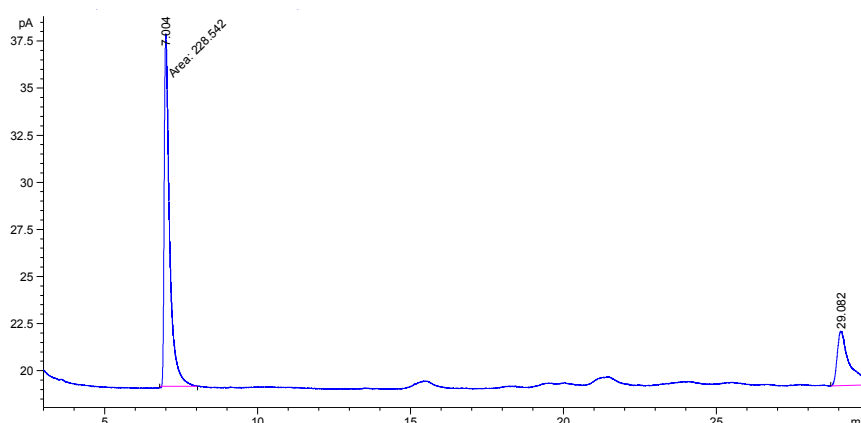


**Figure 30:** Injection of 1  $\mu\text{L}$  of a (E/Z)-**12** 200  $\mu\text{M}$  solution in a Cyclosil-B column from Agilent. The internal standard peak is at 7 min, while the E or Z form of citral comes out after 29 min.

The program was 70°C, hold 1 min and 1°C/min to 90°C with a final hold of 9 min to a total run time of 30 min. The injector and detector temperatures were 180 and 310°C respectively. The split was adjusted to 1:1 in order to allow an amount between 20 and 50 ng of compound to be injected in the system. The flow rate was kept constant at 4 mL/min (71 cm/s). However, the separation was not sufficient to get both forms of the citral, plus the peak had a strong tailing.

In order to fix these issues, the initial temperature was raised to 80°C and the slope to 2.5°C/min to a final temperature of 130°C. As the initial retention time was long, setting up a high slope should allow a faster elution of the compound. The other parameters were not changed. Chromatogram is shown in figure 31.

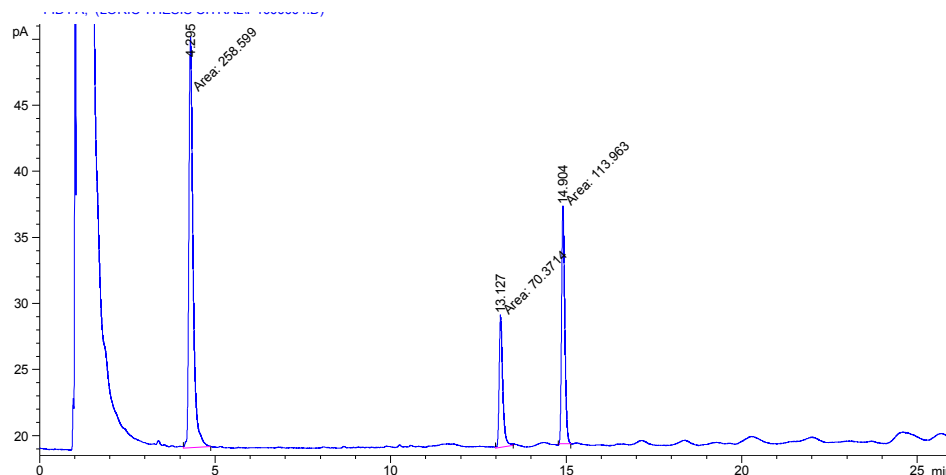


**Figure 31:** Injection of 1  $\mu\text{L}$  of a (E/Z)-12 200  $\mu\text{M}$  solution in a Cyclosil-B column from Agilent. The internal standard peak is at 4.2 min, while one of the E or Z form from citral comes out after 13.1 and 14.9 min. The program was 80°C as starting temperature, then 2.5°C to 130°C, hold 10 min.

The separation of the two forms of citral worked with a good resolution.

Then, (S/R)-13 were injected separately in the column with the same program as for the figure 32. (S)-13 had a retention time of 9.018 min, while (R)-13 had a retention time of 9.057 min. As expected, the mixture of the enantiomers gave a single peak, as showed in figure 32.

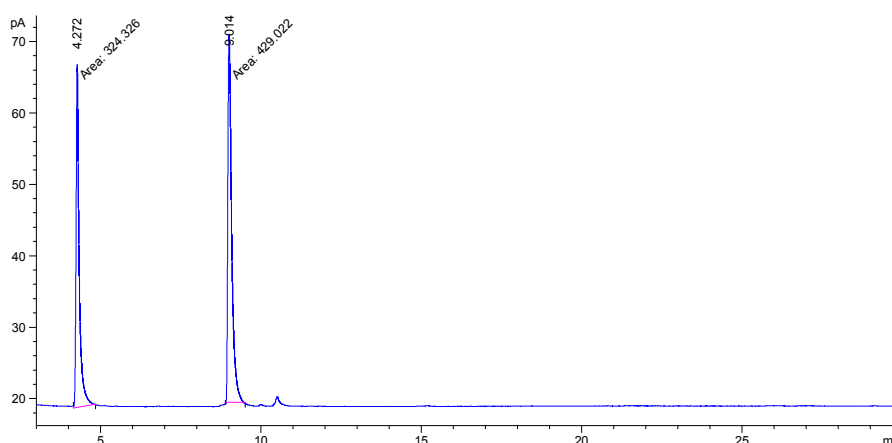


**Figure 32:** Injection of 1  $\mu\text{L}$  of a (R/S)-13 mixture solution at 200  $\mu\text{M}$  in a Cyclosil-B column from Agilent. The internal standard peak is at 4.2 min, while the enantiomeric mixture comes out after 9.014 min. The program was 80°C as starting temperature, then 2.5°C to 130°C, hold 10 min.

Several methods were tried in order to allow the separation of (*S/R*)-13. First, in order to slow the progress of the components in the column, the flow rate was decreased to 2 mL/min (46 cm/s), it did not work and only resulted in thicker peaks. A higher temperature slope could make one of the enantiomer to travel faster, so it was increased to 6°C/min between 80 and 130°C. This method gave shorter retention times but it did not improve the resolution between the two enantiomers. A higher starting temperature was tried with a program going from 120 to 180°C with a 5°C/min slope, except a shorter retention time, still no change was noticed in the separation of (*S/R*)-citronellal.

A method from the literature, from Müller *et al.*[26] paper was tried, even though the column was not the same. The program used was starting at 90°C and hold 45 min, then 5°C/min to 120°C and 40°C/min to 200°C and hold 5 min. The injector and detector were set at 240 and 250°C respectively. The flow rate of hydrogen was adjusted at 1.15 mL/min. This method gave thicker peaks and a column bleeding at the end of the program (figure 33), still no change in the separation of the enantiomers.

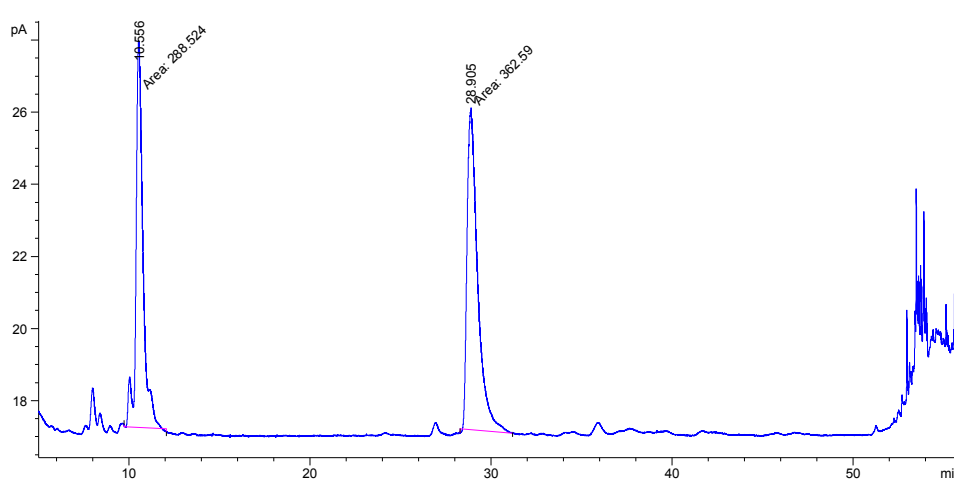


**Figure 33:** Injection of 1  $\mu$ L of a (*R/S*)-13 mixture solution at 200  $\mu$ M in a Cyclosil-B column from Agilent. The internal standard peak is at 10.5 min, while the enantiomeric mixture comes out after 28.9 min. The program was the same as used in the Müller *et al.* paper [26].

Another method from the literature was tried using the *Lorenzo et al.* [36] paper even though the column used was not the same as the one used in the given method. The program was starting at 45°C and holding 6 min, then 2°C/min to 90°C and hold 20 min, then 2°C/min to 180°C and hold 10 min. Injector and detector were set at 230 and 280°C respectively. A constant front pressure of 110 kPa was used, which corresponds to a 6.2 mL/min (26 cm/s) flow. As shown by the figure 34, this method did not improve the quality of the separation.

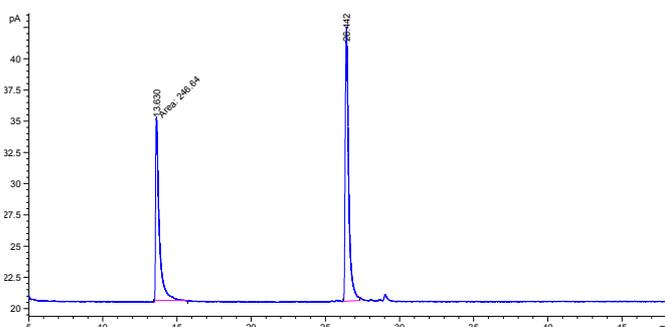


**Figure 34:** Injection of 1  $\mu$ L of a (R/S)-13 mixture solution at 200  $\mu$ M in a Cyclosil-B column from Agilent. The internal standard peak is at 13.6 min, while the enantiomeric mixture comes out after 26.4 min. The program was the same as used in the *Lorenzo et al* paper [36].

Another way to evaluate a mixture of enantiomers would be with rotation of light measurements. This possibility was investigated but it could not be used in this case. Indeed, a concentration is needed for polarimetry measurements. As it is not yet possible to separate the enantiomers, it is not possible to quantify them.

Because of planning issues, further GC programs or techniques could not be tested in order to separate the (S/R)-13 mixture. Thus, it was decided that only conversions rate would be calculated from the consumption of the starting material. Because (E/Z)-12 were not commercially available, it was not possible to identify the peaks in the chromatograms. Therefore, conversion rates are calculated from the differences between the sums of the areas between both (E/Z)-12 peaks. Starting concentration used in the enzymatic assay will be 600  $\mu$ M because the extraction of (E/Z)-12 from buffer A with ethyl acetate yielded to 30%. A first assay with 600  $\mu$ M of (E/Z)-citral and 1  $\mu$ M of WT OYE1 gave a full conversion after 180 min. Time points were fixed to 0/30/45/60/90 min in order to have the most representative use of the substrate.

Figure 35 shows evolution of relative concentrations over time. No product was detected for variants cp303 and cp303W116I. Hence, their concentration is relative to the average concentration of (*E/Z*)-12 at  $t = 0$  min.

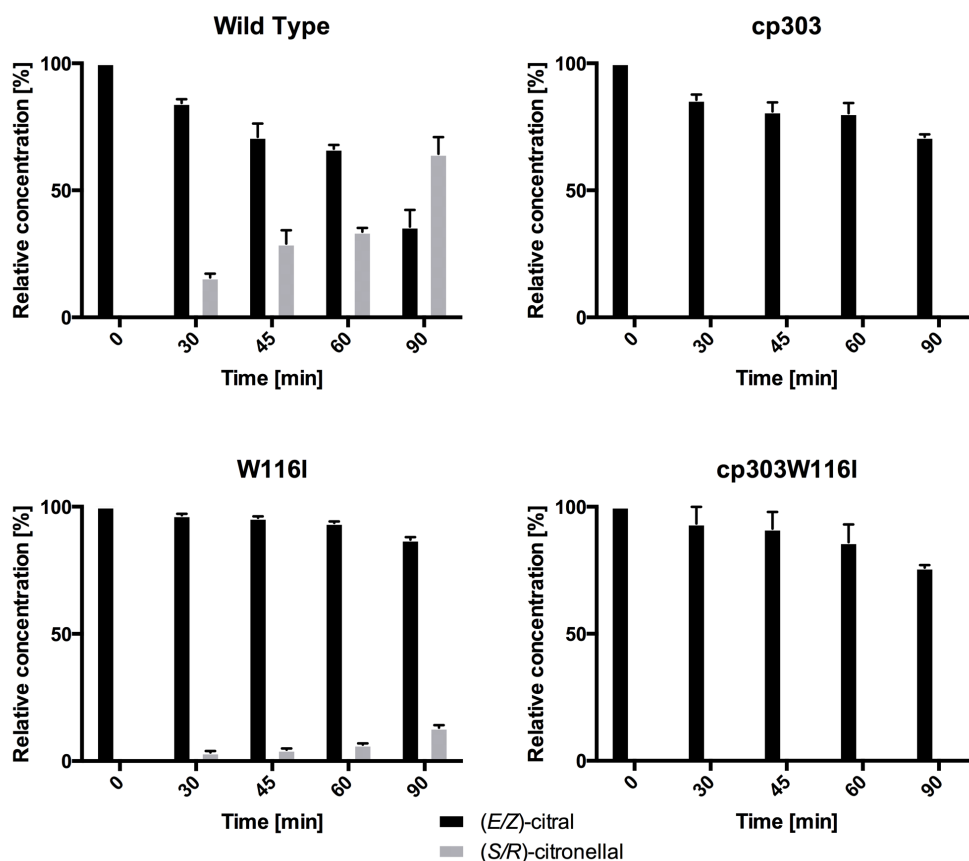


**Figure 35:** Conversion (*E/Z*)-citral into *S/R*-citronellal by WT and its variants. Experiments are done in buffer A (20 mM NaCl, 40 mM Tris-HCl, pH 8 at 20°C) with 600  $\mu\text{M}$  of (*E/Z*)-12 as starting material using phosphite dehydrogenase and NaPi as cofactor regenerating system

Table 12 shows conversion rates for (*E/Z*)-citral.

**Table 12:** Conversion rate expressed as  $\left[\frac{\mu\text{M}_S}{\text{min}\cdot\text{nmol}_E}\right]$  for each variant with (*E/Z*)-citral as substrate.

Enzyme	Conversion Rate
Wild Type	$29.3 \pm 1.8$
cp303	$8.1 \pm 0.9$
W116I	$9.6 \pm 0.7$
cp303W116I	$5.8 \pm 0.7$

## 6. Discussion

### 6.1 (*S*)-carvone

As Stewart reported [2], W116I mutant showed reversed enantioselectivity with an *ee* (*S*) of 91% for (*S*)-**1** compared to WT possessing an *ee* (*R*) of 91%. The substitution of Trp at position 116 positions (*S*)-carvone in a flipped conformation compared to WT. It was also reported that the Trp replacement enables the isoprenyl substituent of (*S*)-**1** to adopt a different conformation due to the substitution of Trp to a smaller amino acid, as shown in figure 36.

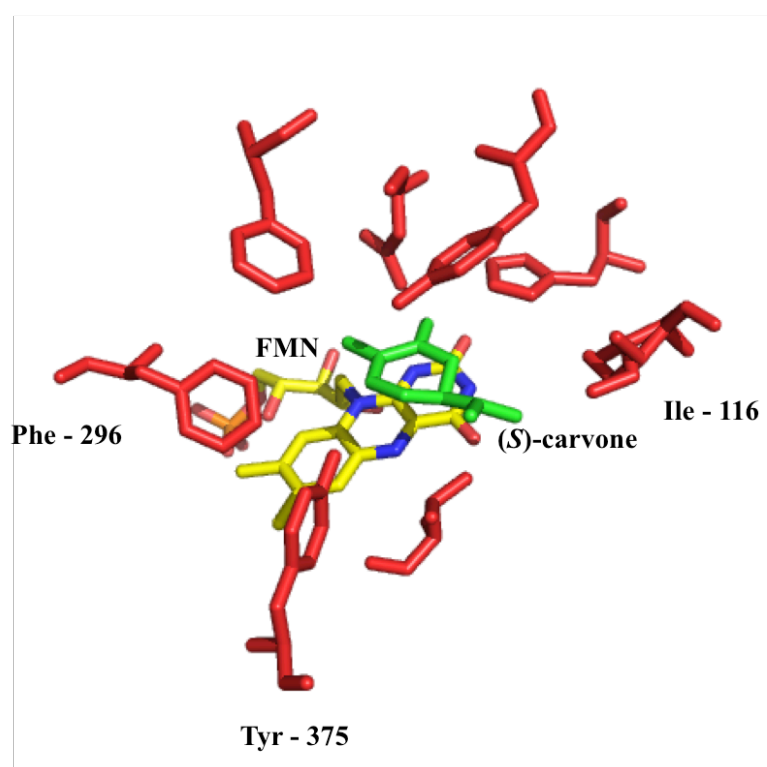


**Figure 36:** Position of *S*-**1** in the active site of W116I. Replacement of Trp-116 by Ile allows (*S*)-**1** to bind in a flipped conformation compared to WT. Residues in the active site pocket are the same as in figure 1.

While a molecule may bind in many different conformations, not all binding events are catalytically productive. One can reason, the W116I mutation alters the active site, and increases enzyme performance (almost 5x faster than WT), due to more productive binding events. (*S*)-**1** enters the W116I mutant in the flipped conformation (compared to WT), which is optimal for the reduction chemistry. Thus it is resulting in a faster conversion for flipped (*S*)-**1** thus more (*S/S*)-**2** is produced than (*R/S*)-**2**. The same phenomenon may happen for WT, but in this case, the positioning of the (*S*)-carvone in the original conformation is converted faster than when it is positioned in a flipped conformation, resulting in an enantioselectivity of 91% for (*R/S*)-**2**.

For the circular permutant (cp303), the conversion rate was faster than WT by 2x. As stated by *Daugherty et al.* [1], this permutant had an increased reductive-half reaction rate, which allows faster FMN cofactor regeneration. Regarding the permutant's enantioselectivity, an *ee* of 79% for (*R/S*)-**2** was calculated. In addition to the preserved *R*-enantioselectivity, an overall performance increase was observed in cp303 as stated in previous work [1].

The last mutant, cp303OYEW116I showed a conversion rate 3.6x higher than WT OYE1 and nearly identical to OYEW116I. The enantioselectivity did not switch from (*R/S*)-**2** to (*S/S*)-**2**, as expected. Instead, an *ee* of 88% for (*2R/5S*)-carvone was calculated. The W116I enantioselectivity improvement was expected to transfer to the cp303 permutant. However the original WT preference was observed, at an improved rate. By cutting the loop in the region VI (amino acids from 289 to 309 [37]), the Phe-296 is absent in cp303, modifying substrate binding. It is possible that the isoprenyl substituent is in the vacant position near Phe-296. In order to get more data about the substrate binding mode, further studies are necessary.

## 6.2 (*R*)-carvone

As previously stated by *Padhi et al.* [2], the enantioselectivity for (*R*)-**1** did not switch with W116I and resulted in an *ee* > 99% (*R/R*)-**2**. The same selectivity was found for all the OYEs tested in this work.

As shown in figure 37 and from these results, tryptophan does not play an important role in the positioning of (*R*)-**1** in the active site, as it is the case for (*S*)-**1**. However, differences in conversion rates were observed. Even though W116I did not show a reversed enantioselectivity, its conversion rate was higher than the WT by 1.6x, however is not as significant for efficient catalysis of (*R*)-**1**. However, since the rate is higher without tryptophan, it may be possible that Trp-116 stereochemically impedes the positioning of (*R*)-**1** in the active site of WT.

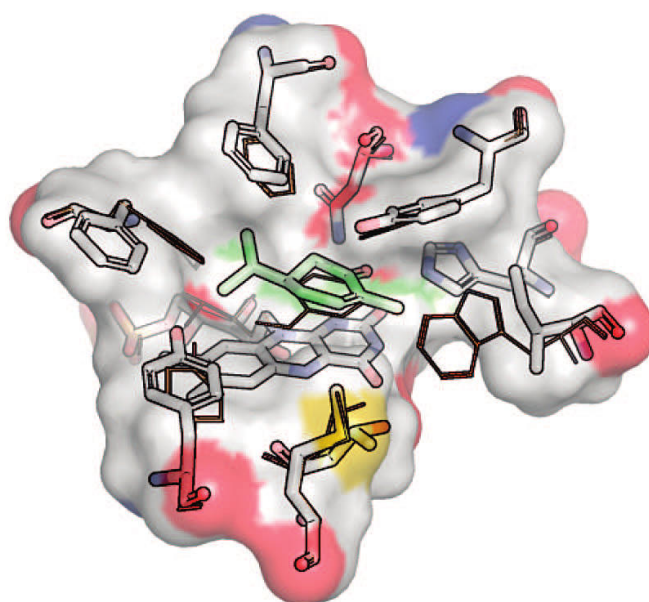


**Figure 37:** Induced fit docking of (*R*)-**1** with W116I. Some residues of the active site are shown in ball and stick form. Light green molecule is the (*R*)-carvone in its most favorable complex. Depicted black sticks show the experimental structure of WT. Figure from *Padhi et al.* [2]

The conversion rate with cp303 was 2x lower than the wild type. According to figure 37, it can be supposed that the loop VI region is important in the stabilization of the substrate in the active site. The isoprenyl substituent of (*R*)-carvone is orientated towards Phe-296, which is absent in the cp303 variant. Without this part of the loop, it is possible that (*R*)-1 cannot effectively bind the FMN cofactor.

The cp303W116I variant showed the highest conversion rate (table 8): it was 2.1x higher than WT. This result shows that even if loop VI is cut, (*R*)-1 can still be more efficiently catalyzed. As seen before, Phe-296 is missing in this mutant, thus the substrate should not bind effectively in the active site, however improved activity was observed. It is possible that the substitution in addition to the CP force a new positioning of (*R*)-carvone. It can be suggested that the isoprenyl substituent of (*R*)-1 could be placed in the supplementary hydrophobic pocket (as showed in figure 36) and that the high rate could be a consequence of the rapid diffusion of (*R*)-1 into the active site due to the increased entrance. However, further investigations are required.

### 6.3 *Trans* $\alpha$ -methylcinnamaldehyde

All investigated OYEs yielded same product, without any switch in enantioselectivity, catalyzing the transformation of **3** into (*S*)-**4** with an *ee* > 99%.

Concerning the catalytic rates, WT had the fastest, cp303 and W116I equally suffered 10% loss in activity, while cp303W116I lost 40%. Changes in structure may explain these differences. A previous study by *Stueckler et al.* [35] showed how **3** is positioned in the active site of OYE from *S.cerevisiae* (figure 38). Even though it is not exactly the same enzyme, a major part of the components in the active site are conserved among species. Thus, it can be used for comparison purposes.

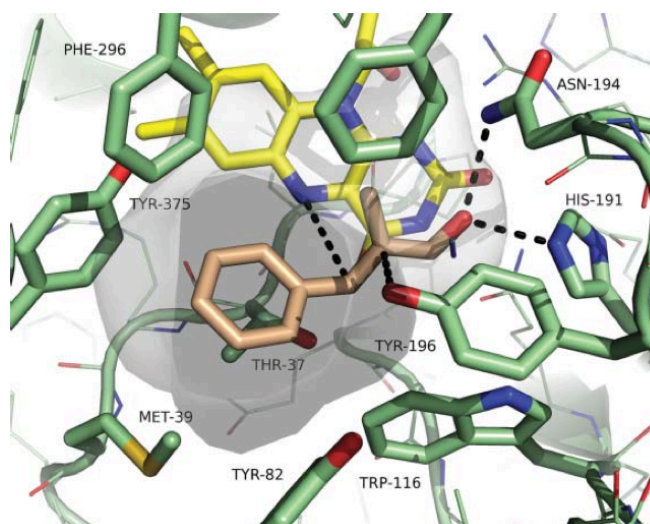


**Figure 38:** Active site of OYE from *S.cerevisiae*. Amino acids side chains are shown in green. FMN is in yellow. Dashed lines from **3** represent hydrogen bonding interactions with the cofactor, Asn-194 and His-191. The line between Tyr-196 and **3** represent a close contact (3.4 – 3.8 Å). Figure from *Stueckler et al.* [35]

As shown by the previous figure, the aromatic ring of **3** binds above Thr-37 suggesting no interactions with Trp-116. The substrate lies above FMN, mainly interacting with His-191 (Massey stated this position has an important role in hydrogen bond formation with phenolic compounds [11]), Asn-194 and Tyr-196. Substituting the tryptophan for isoleucine in W116I slightly reduces the conversion rate by 12%. Trp-116 seems to not interact in a significant way in the positioning of **3**. Changing this amino acid to an Ile and enlarging the active site does not seem to be useful. It is possible **3** has less interactions with the cofactor, thus more time is needed for reduction. The indole ring of Trp-116 might be useful in keeping the molecule as it is in figure 38.

The circular permutant cp303 truncated loop VI containing Phe-296, resulting in a 10% decrease in conversion rate compared to WT. The flexibility conferred to this permutant did not seem beneficial to active site interactions for **3**, having a similar rationale to W116I. Even if Phe-296 does not interact with **3**, the loop truncation may slightly perturb the efficient binding of **3** into the active site.

Mutant cp303W116I possesses both previously mentioned changes in its structure, and understandably had similar lower catalytic rates. Substituting Trp-116 and truncating VI loop may enable catalytically unproductive flexibility for interactions with **3**, explaining reduced activity.

Since no enantioselectivity switch was observed, it is suggested that the modifications made to OYE did not have an effect on the positioning of **3** in the active site as (*S/R*)-**1** did. It is possible the other active site substitutions would alter orientation of **3** to improve enantioselectivity and/or the catalytic rate.

## 6.4 Myrtenol

The reduction of **5** by the OYE wild type and the variants tested was not successful. The starting material was not consumed after 24 hours with WT. The variants, cp303, W116I and cp303W116I also did not show any consumption of the starting material after 6 hours. *Goretti M. et al.* [38] hypothesized a metabolic pathway for the reduction of (*R*)-myrtenal within a whole cell system (figure 39).

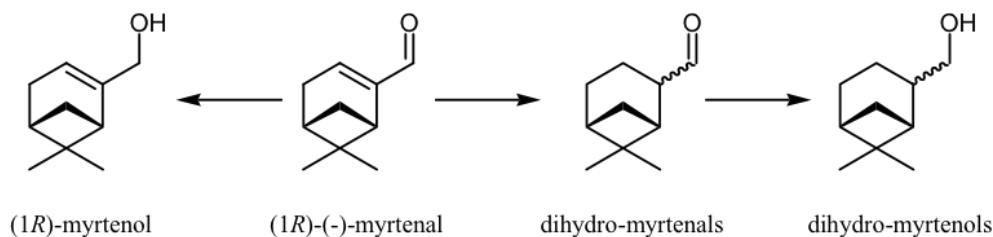


**Figure 39:** Metabolic pathway of (*R*)-myrtenal used as substrate with a whole cell system involving non-conventional yeast cells. Figure by *Goretti M. et al.*[38]

According to this figure, **5** cannot lead to the (*S/R*)-**6** as expected. This is only possible if the alcohol functional group was first oxidized into an aldehyde, thus reducing the double bond of OYE is possible before the ketone is reduced into an alcohol. Such transformations are possible in a whole cell system because of the presence of many different enzymes.

Such transformations are possible in whole cell systems, because of the presence of other enzymes. However, since **5** was not consumed by the OYEs investigated in this work can bring positives arguments to the assumptions made for in this pathway.

An alternative experiment would be the transformation from (*R*)-myrtenol to (*S/R*)-**6** in a one-pot, three step reaction, by adding an aldehyde and alcohol dehydrogenases to the system. These enzymes would be able to oxidize the alcohol into an aldehyde, allowing the reduction of the double bond by OYE1 before the aldehyde dehydrogenase reduces the functional group back to an alcohol.

### 6.5 Methyl 2-hydroxymethylacrylate

Conversion rate for **7** was the slowest observed in this work. Only WT was investigated, at a 5x higher concentration than usual, and it gave a rate of  $0.7 \left[ \frac{\mu M_s}{min \cdot nmol_E} \right]$  with an enantioselectivity of >99% for (*R*)-**8**.

A previous study done by *Stueckler et al.* [8] also showed a slow conversion with OYE1. It converted 7% of 10 mM **7** over 24 hours at 30°C with NAD<sup>+</sup> as cofactor and a glucose dehydrogenase recycling system, resulting in an observed conversion rate of  $0.35 \left[ \frac{\mu M_s}{min \cdot nmol_E} \right]$ . However, the difference between the two conversion rates could be due to the fact that Stueckler's reaction was done at 30°C and with NAD<sup>+</sup> as cofactor. Studies have been done about the difference in affinity between NADH and NADPH for WT. Results (Lutz unpublished data) showed that  $K_{M,NADPH}$  was 70x lower than  $K_{M,NADH}$ , thus even at higher reaction temperatures, the rate obtained by Stueckler is lower than the one obtained in this present work. Because of the cofactor difference and the temperature change, a direct comparison of conversions rates is difficult to assess.

Stueckler also showed that using a modified **7** did not improve the conversion for OYE1. Three derivatizations of **7** (allyl, benzyl and a tert-butyldimethylsilylto) on the single bonded oxygen of the carboxylic acid (see **7** in figure 4) were done. O-allyl-**7** gave 5% conversion after 24 hours, while O-benzyl-**7** and O-tert-butyldimethylsilyl-**7** gave 3 % and non-detectable amounts respectively. These results show that the structure of **7**, even modified, is not optimal for the active site of OYE1. In order to increase the conversion rate of OYE1 with **7**, it may be advantageous to focus studies on optimizing the shape of the active site.

### 6.6 4-phenyl-3-butyn-2-one

No switch in enantioselectivity was observed all OYEs tested gave >99% (*Z*)-**10** enantioselectivity from the conversion of **9**. However, diverse conversion rates were obtained for the first reduction on **9**. The highest was with WT. Next was cp303, which showed half of WT's rate, while W116I was a bit more efficient with a reduction of 26% compared to wild type. The worse case was with cp303W116I, which showed an activity lowered by 93% from the WT.

These results show that increasing the active site volume by removing Trp-116 has reduced the conversion rate. It is possible that tryptophan's indole ring was interacting with the substrate, stabilizing its position above the FMN cofactor

A similar rational can be made with the cp303 mutant. When the loop VI is truncated, the conversion rate is reduced by half meaning that the amino acids removed were interacting in some ways with **9** and helping in the bioreduction process. A flat and rigid substrate like **9** needs to be held properly in order to be reduced by OYE1. Changing the active site did not result in an improvement in catalysis. It can be stated that allowing too much freedom for the substrate movement is not helpful in the case of a flat molecule. A similar tendency was observed with **3**.

An argument can be made that cp303W116I has the most freedom for the **9** into the active site. This mutant showed additive properties regarding the conversion rate. By taking both mutations from cp303 and W116I for **9**, this enzyme showed a poor conversion rate.

The second step, involving the reduction of (*E/Z*)-**10** into **11** showed overall lower conversion rates than with the first step. At this point, a first assumption can be made by saying that the affinity of the enzyme for **9** is higher than for (*E/Z*)-**10**. The tendency for decreased catalytic rates for each enzyme followed the one stated previously for the conversion of **9** to (*E/Z*)-**10**, thus same conclusions can be made.

## 6.7 (*E/Z*)-citral

WT and W116I mutant were the only enzymes with detectible product formation. The two other OYEs, cp303 and cp303W116I consumed (*E/Z*)-**12**, however no (*S/R*)-**13** was detected. No enantioselectivity could have been determined for (*E/Z*)-**12** because reference molecules were not commercially available. However, conversion rate can be discussed. Native OYE1 gave the highest conversion rate, meaning that the modifications done on the structure of OYE1 were not helpful in any way for the bioreduction of (*E/Z*)-**12**.

*Padhi et al.* tested (*E/Z*)-**12** with W116I and did not report a significant conversion over time [2]. In this work, this mutant was converted to (*E/Z*)-citral 68% slower than WT OYE1, which is supported by previous studies. The cp303 OYE1 was less efficient by 73% compared to WT. These two mutants showed that the modifications in the active site perturbed the efficiency of the catalysis. Citral is also a flat molecule like **3** and **9**, meaning that the previous statements made for these molecules can also be applied with (*E/Z*)-**12**.

As expected, cp303W116I showed additives properties with a significantly lower conversion rate, which was 81% lower than WT. Opening the active site with cp303 and removing Trp-116 with W116I led to changes that probably perturb the positioning of (*E/Z*)-**12** into the active site.

## 7. Conclusion

With the exception of myrtenol, which was not consumed by any enzymes tested, and methyl 2-hydroxymethylacrylate, which was giving very slow conversion rates, this work permits a synopsis of the general behavior for the OYEs mutants tested. Indeed, except for **(S/R)-1**, the variants did not show any switch in enantioselectivity or better conversion rates than WT.

W116I is a mutant where Trp-116 is replaced by an Ile, allowing access to a hydrophobic pocket, while cp303 is an enzyme where the loop VI is truncated, allowing greater enzyme flexibility as well as a bigger active site entrance. When both modifications were united into cp303W116I, the active site has the biggest volume from all the other variants, in addition to an increased flexibility. All planar substrates, like *trans*  $\alpha$ -methyl-cinnamaldehyde, 4-phenyl-3-butyn-2-one and (*E/Z*)-citral gave the same tendency among the conversion rates obtained. For all of these molecules, WT obtained the best rates, while W116I and cp303 were not significantly different from each other but always lower than WT when cp303W116I, showed additives properties by consistently giving the worse conversion rates.

In a general view, it can be hypothesized that for planar molecules the changes made allowed a degree of freedom in the active site that was prohibiting effective catalysis. These substrates may need an active site that orients them specifically over the FMN cofactor in order to allow an efficient reduction.

For **(S)-1**, W116I showed a reversed enantioselectivity with an enantiomeric excess of 91% for **(S/S)-2** as well as the highest catalytic rate for this substrate. A possible cause for this high rate is that the flipped conformation in which **(S)-1** was binding in W116I was also more optimal than the natural binding mode thus switching the enantioselectivity. However, this switch was not observed with **(R)-1**, even though the conversion rate was the highest with W116I, and suggested a more optimal positioning of (*R*)-carvone over FMN. The circular permutant cp303 gave a higher conversion rate than the wild type but always lower than W116I for **(S/R)-1**, this mutant did not changed the enantioselectivity. Finally, cp303W116I showed a conversion rate close to the W116I for **(S)-1**, while it was the highest for **(R)-1**, supposing that the huge active site entrance was allowing **(R)-1** to take a conformation that is significantly more optimal than with WT. However, this last mutant did not show any change in enantioselectivity for both **(S/R)-1**.

The results presented above suggest that it would be beneficial to investigate substrates that are more “carvone-like”, for example: 2-methyl-2-cyclohexenone, perillaldehyde or cyclohexenone. These compounds could help give additional credit to the arguments about W116I and cp303 (as well as cp303W116I) being better designed to give enhanced responses with stereochemically occupied molecules while planar substrates would display decreased efficiency. The myrtenol was one of the molecules that could give interesting results concerning the substrate positioning. The conversion of myrtenol could also if it is used with other enzymes in order to follow the pathway suggested by *Goretti et al.* [38]. Finally, in depth kinetic data ( $K_m$ ,  $V_{max}$ ) could be determined by using different concentrations of enzyme in order to have a better understanding and complementary information about the mutant's catalytic activity.

## 8. Acknowledgements

I would like to take the opportunity to thank a few people who helped me through this scientific journey.

Firstly, I want to thank my father, Petruzzi Francesco and my mother, Petruzzi Cinzia, who were always there to support me. They helped me to take advantage of an unique opportunity to improve myself through an unforgettable international professional experience. I am forever grateful towards them for allowing me to learn a lot of new things about science and myself.

I want to thank my close friends who gave me motivation when I needed it. Leaving home for a long time is never easy, but friendship can always help to make painful things better.

Next, I have to express my deepest appreciation to Vial Christian, who helped me with his knowledge about the Gas Chromatography. I think that I would have lost a lot of time without him. Thank you.

A big thanks to Dr. Crelier Simon, Iamurri Samantha, Jenkins Matt, Quertinmont Leann and Muthu Pravin for your help, presence and feedback for my thesis. It helped me better myself as well as doing a better job. I would not have been able to write something this important without your help.

Of course, I want to give Dr. Orrù Roberto a big thank you. He instructed and helped me with theoretical as well as practical stuff during my whole stay here. Without his guidance and these very nicely built discussions, this entire work would not have been the same. Through his knowledge about the Old Yellow Enzyme and crystallography, he guided me in order to make me think about the right things while never forgetting to give me helpful feedback.

Next, I want to express my deepest gratitude to Prof. Lutz Stefan, who allowed me to dive into the academic research in his group at Emory University. It was the greatest experience of my life so far, and I learned a lot about science and research thanks to him. I deeply appreciate the opportunity he gave me to improve myself through this challenging work. I thank him for receiving me and allowing me to work with his group for my bachelor thesis. It was an unforgettable experience.

Most of all, I want to thank Dr. Pfeifer Marc. Without him, none of this would have been possible. I thank him for giving me the incredible opportunity to travel to the USA for my bachelor thesis, which was one of my biggest hopes. He opened the door in front of me, allowing me to take all of these chances for my scientific career. Thank you for your consistently motivating attitude, which I appreciate, and thank you for your support, and for the helpful feedback you always give me.

Again, thank you all.

Emory University, 08.21.14, Petruzzi Loric

## 9. Literature

1. Daugherty, A., S. Govindarajan, and S. Lutz, *Improved biocatalysts from a synthetic circular permutation library of the flavin-dependent oxidoreductase old yellow enzyme*. J Am Chem Soc, 2013. **135**: p. 14425-14432.
2. Padhi, S.K., D.J. Bougioukou, and J.D. Stewart, *Site-Saturation Mutagenesis of Tryptophan 116 of Saccharomyces pastorianus Old Yellow Enzyme Uncovers Stereocomplementary Variants*. J Am Chem Soc, 2009. **131**: p. 3271-3280.
3. Nguyen, L.A., H. He, and C. Pham-Huy, *Chiral drugs : an overview*. Int J Biomed Sci, 2006. **2**: p. 85-100.
4. Kim, J.H. and A.R. Scialli, *Thalidomide: the tragedy of birth defects and the effective treatment of disease*. Toxicol Sci, 2011. **122**: p. 1-6.
5. Battistel, E., et al., *Enzymatic Resolution of (S)-(+)-Naproxen in a Continuous Reactor*. Biotechnol Bioeng, 1991. **38**: p. 659-664.
6. Reihold, F.D., et al., *Synthesis of L-a-Methyldopa from Asymmetric Intermediates*. The Journal of Organic Chemistry, 1967. **33**: p. 1209-1213.
7. Winkler, C.K., et al., *Asymmetric bioreduction of activated alkenes to industrially relevant optically active compounds*. Journal of Biotechnology, 2012. **162**: p. 381-389.
8. Stueckler, C., et al., *Asymmetric Synthesis of (R)-3-Hydroxy-2-methylpropanoate ('Roche Ester') and Derivatives via Biocatalytic C-C-Bond Reduction*. Advanced Synthesis & Catalysis, 2010. **352**(14-15): p. 2663-2666.
9. Bhatt, M.R. *Future Prospects of Enzyme Engineering*. Scribd 2009 27/08/2009; 1-21]. <http://fr.scribd.com/doc/24990319/Future-Prospects-of-Enzyme-Engineering>.
10. Massey, V. and R.M. Kohli, *The Oxidative Half-reaction of Old Yellow Enzyme: THE ROLE OF TYROSINE 196*. The Journal of Biological Chemistry, 1998. **273**: p. 32763-32770.
11. Massey, V., et al., *On the Active Site of Old Yellow Enzyme - ROLE OF HISTIDINE 191 AND ASPARAGINE 194*. The Journal of Biological Chemistry, 1998. **273**: p. 32753-32762.
12. de Carvalho, C.C.C.R. and M.M.R. da Fonseca, *Carvone: Why and how should one bother to produce this terpene*. Food Chemistry, 2006. **95**: p. 413-422.
13. Porto, C., et al., *(R)-(-)-Carvone and (1R, 4R)-trans-(+)-Dihydrocarvone from Poirertia latifolia Vogel*. J. Braz. Chem, 2010. **21**: p. 782-786.
14. Dong, Y., et al., *The structure and antimalarial activity of dispiro-1,2,4,5-tetraoxanes derived from (+)-dihydrocarvone*. Bioorganic & Medicinal Chemistry Letters, 2010. **20**: p. 6359-6361.
15. Jacquot de Rouville, H.-P., et al., *Synthesis and analytical resolution of chiral pyrazoles derived from (5R)-dihydrocarvone*. New Journal of Chemistry, 2009. **33**: p. 293-299.

16. Krawczyka, H., et al., *Asymmetric synthesis of enantiomerically pure 7-isopropenyl-4a-methyl-3-methyleneoctahydrochromen-2-ones*. *Tetrahedron: Asymmetry*, 2007. **18**: p. 2712-2718.
17. Roy H.Valentine, H.A.B., *Process for the preparation of dihydrocinnamaldehyde derivatives*. 1981: United States.
18. Clemens Stueckler, et al., *Bioreduction of  $\alpha$ -methylcinnamaldehyde derivatives: chemo-enzymatic asymmetric synthesis of Lilial and Helional*. *The Royal Society of Chemistry*, 2010. **39**: p. 8472-8476.
19. Scriabine, I., *Aldehydes useful in perfumery*, R.P. Sa, Editor. 1970: United States of America.
20. S.P. Bhatia, et al., *Fragrance material review on myrtenol*. *Food and Chemical Toxicology*, 2008. **46**: p. S237-S240.
21. Cohen, N., et al., *Synthetic Studies on (2R, 4'R, 8'R)- $\alpha$ -Tocopherol. An Approach Utilizing Side Chain Synthons of Microbiological Origin*. *Journal of Organic Chemistry*, 1976. **41**: p. 3505-3511.
22. Quirico, B. and F. Albert, *Eine chiral ökonomische Totalsynthese von (R)- und (S)-Muskon via Epoxysulfoncyclofragmentierung*. *Helvetica Chimica Acta*, 1977. **60**: p. 925-944.
23. Evans, D.A., et al., *Polyether antibiotics synthesis. Total synthesis and absolute configuration of the ionophore A-23187*. *J Am Chem Soc*, 1979. **101**: p. 6789-6791.
24. Kirkham, J.E.D., V. Lee, and J.E. Baldwin, *Biomimetic synthesis of marine sponge metabolite spiculoic acid A and establishment of the absolute configuration of the natural product*. *Chemical Communications*, 2006. **27**: p. 2863-2865.
25. Stürmer, R., et al., *Method for the enzymatic reduction of alkyne derivatives*. 2007, BASF SE: United States.
26. Müller, A., B. Hauer, and B. Rosche, *Asymmetric Alkene Reduction by Yeast Old Yellow Enzymes and by a Novel Zymomonas mobilis Reductase*. *Biotechnol Bioeng*, 2007. **98**: p. 22-29.
27. Trasarti, A.F., A.J. Marchi, and C.R. Apesteguía, *Highly selective synthesis of menthols from citral in a one-step process*. *Journal of Catalysis*, 2004. **224**: p. 484-488.
28. Xu, D., R.M. Kohli, and V. Massey, *The role of threonine 37 in flavin reactivity of the old yellow enzyme*. *Proceedings of the National Academy of Sciences*, 1999. **96**(7): p. 3556-3561.
29. Yu, Y. and S. Lutz, *Circular permutation: a different way to engineer enzyme structure and function*. *Trends in Biotechnology*, 2011. **29**(1): p. 18-25.
30. Karplus, P.A., K.M. Fox, and V. Massey, *Flavoprotein structure and mechanism. 8. Structure-function relations for old yellow enzyme*. *The FASEB Journal*, 1995. **9**(15): p. 1518-26.

31. Promega. *BL21(DE3)pLysS Competent Cells*. Visited 2014 06.16.2014; <http://www.promega.com>
32. Novagen, *pET System Manual*. 2003. **10**: p. 11-14.
33. Eisenberg, P., *Cavitation*, in *On the mechanism and prevention of cavitation*. 1950, Navy Dept., David W. Taylor Model Basin, Washington. p. 121-128.
34. Sigma-Aldrich. *Introduction to PAGE-Separation of Proteins Based on Size*. Visited 2014 07.16.2014; <http://www.sigmaaldrich.com>
35. Stueckler, C., et al., *Bioreduction of alpha-methylcinnamaldehyde derivatives: chemo-enzymatic asymmetric synthesis of Lilial and Helional*. Dalton Transactions, 2010. **39**: p. 8472-8476.
36. Lorenzo, D., et al., *Composition and Stereoanalysis of Cymbopogon winterianus Jowitt Oil from Southern Brazil*. Flavour and Fragrance Journal, 2000. **15**: p. 177-181.
37. Pompeu, Y.A., B. Sullivan, and J.D. Stewart, *X-ray Crystallography Reveals How Subtle Changes Control the Orientation of Substrate Binding in an Alkene Reductase*. ACS Catalysis, 2013. **3**: p. 2376-2390.
38. Goretti, B., et al., *Production of Flavours and Fragrances via Bioreduction of (4R)-(-)-Carvone and (1R)-(-)-Myrtenal by Non-Conventional Yeast Whole-Cells*. Molecules, 2013. **18**: p. 5736-5748.

## 10. Appendix

### 10.1 Recipes for reagent used during the experiment

Following recipes are listed in the order of appearance in the text.

Table 13 shows the recipe for the LB and 2YT medium.

**Table 13:** Composition of LB and 2YT mediums used during the transformation and the overexpression respectively.

Component	LB	2YT
Bacto™ Peptone	10 g/L	16 g/L
Yeast Extract	5 g/L	10 g/L
NaCl	10 g/L	5 g/L
pH	7	7

Table 14 shows the recipe for the buffers used during the chromatography steps.

**Table 14:** Composition of the buffers used for the purification of cp303W116I and W116I.

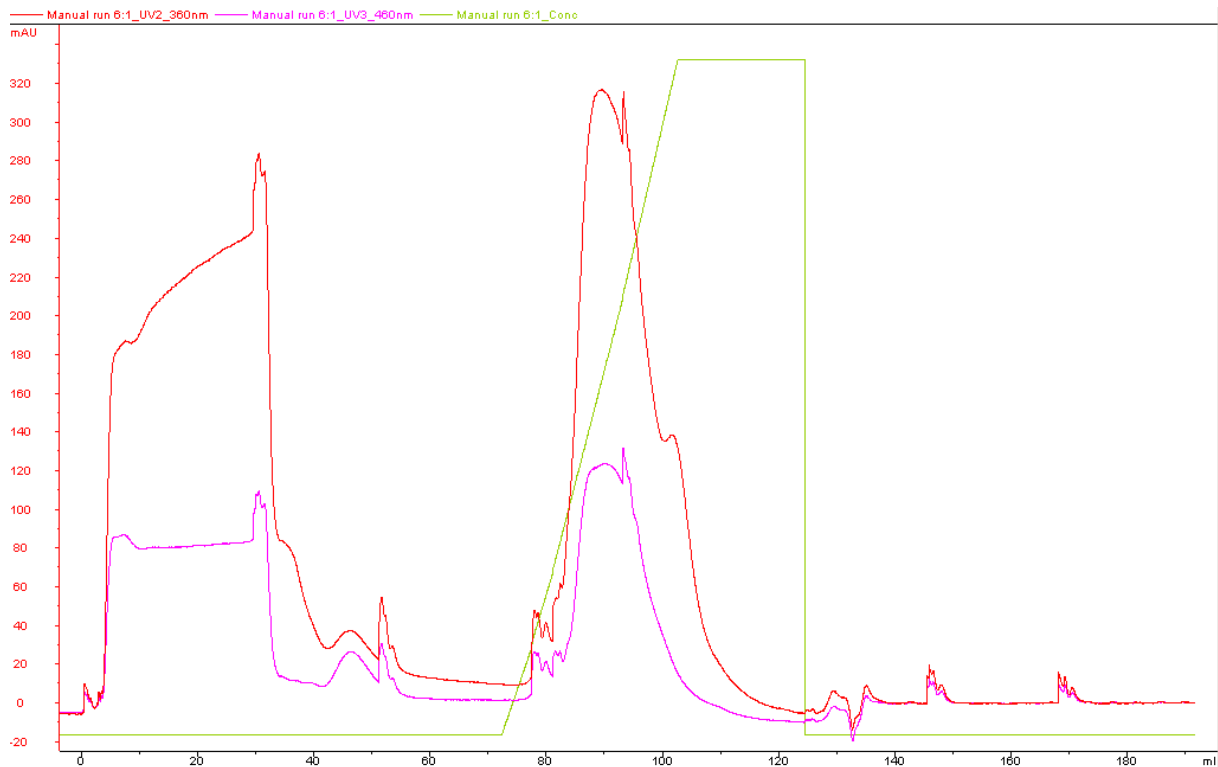
Buffer	Sodium Chloride	Tris Hydrochloride	pH
A	20 mM	40 mM	8
A (desalted)	-	40 mM	8
B	1 M	40 mM	8
C	300 mM	40 mM	8

Table 15 shows the recipe for the making of two SDS gel 10% acrylamide with 0.75 mm plates from BioRad.

*Table 15: Recipe for the preparation of two SDS gel with a final concentration of 10% acrylamide.*

	<b>Reagent</b>	<b>Quantity</b>
Running gel	Deionized water	3.5 ml
	Acrylamide 40%	2 ml
	Buffer 1.5 M Tris, pH 8.8	2 ml
	SDS 10%	80 $\mu$ l
	APS 10%	80 $\mu$ l
	TEMED	8 $\mu$ l
Stacking gel	Deionized water	3.15 ml
	Acrylamide 40%	0.5 ml
	Buffer 0.5 M Tris, pH 8.8	1.25 ml
	SDS 10%	50 $\mu$ l
	APS 10%	50 $\mu$ l
	TEMED	5 $\mu$ l

## 10.2 Anion Exchange Chromatography



**Figure 40:** Anion Exchange Chromatography purification of OYEW116I from cell lysate on a HiTrap Q FF (5 mL) column. The purple line is the OD<sub>460nm</sub>, red line is the OD<sub>360nm</sub>. Green line represents the gradient in percent. Values are given against a volume pumped into the system with a flow rate of 5 mL/min. Injection stands at  $v = 0$  mL. The flow through is between 0 and 50 mL, while the OYEW116I elution begins at ~80 mL.

### 10.3 Size Exclusion Chromatography

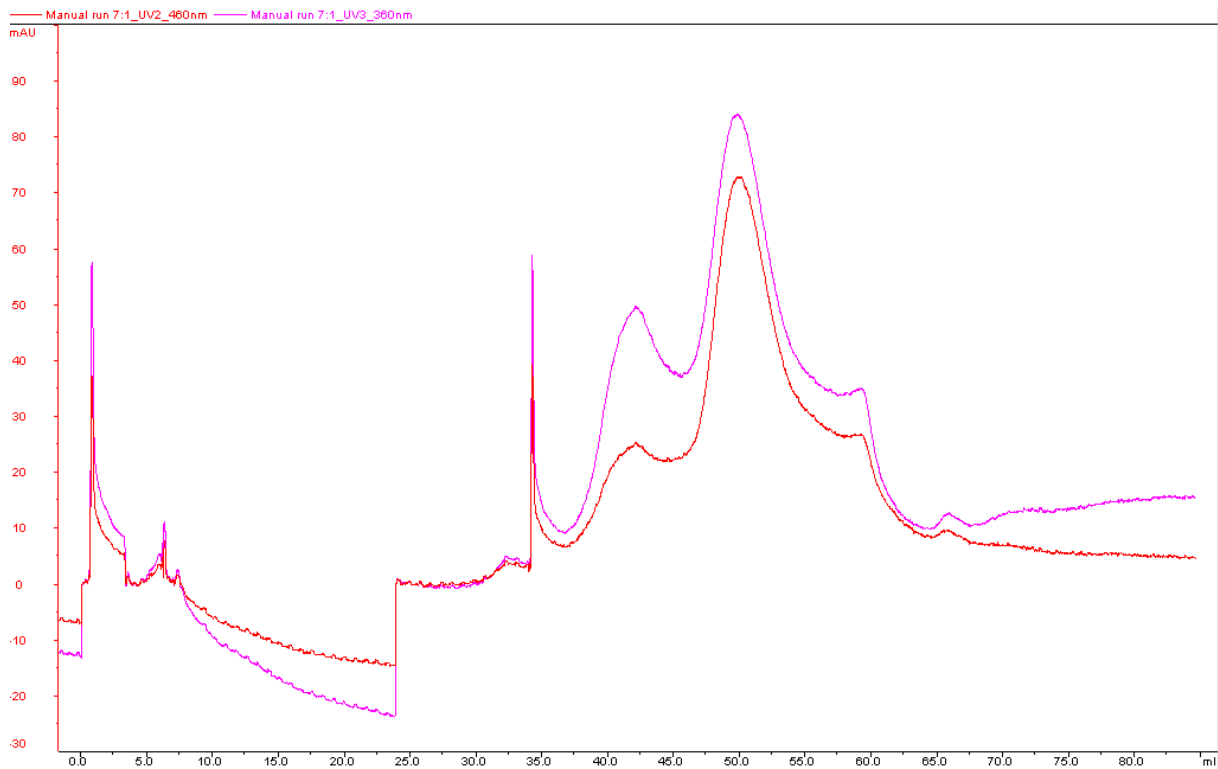


**Figure 41:** Purification of OYEW116I mutant from cell lysate on a HiPrep 16/60 Sephacryl S-100 column (160 mL) with a flow rate of 0.5 mL/min.. The purple line represents the  $OD_{460nm}$ , red line is the  $OD_{360nm}$ . The Injection is at  $v = 0$  mL. Elution of the protein of interest after  $\sim 46$  mL.

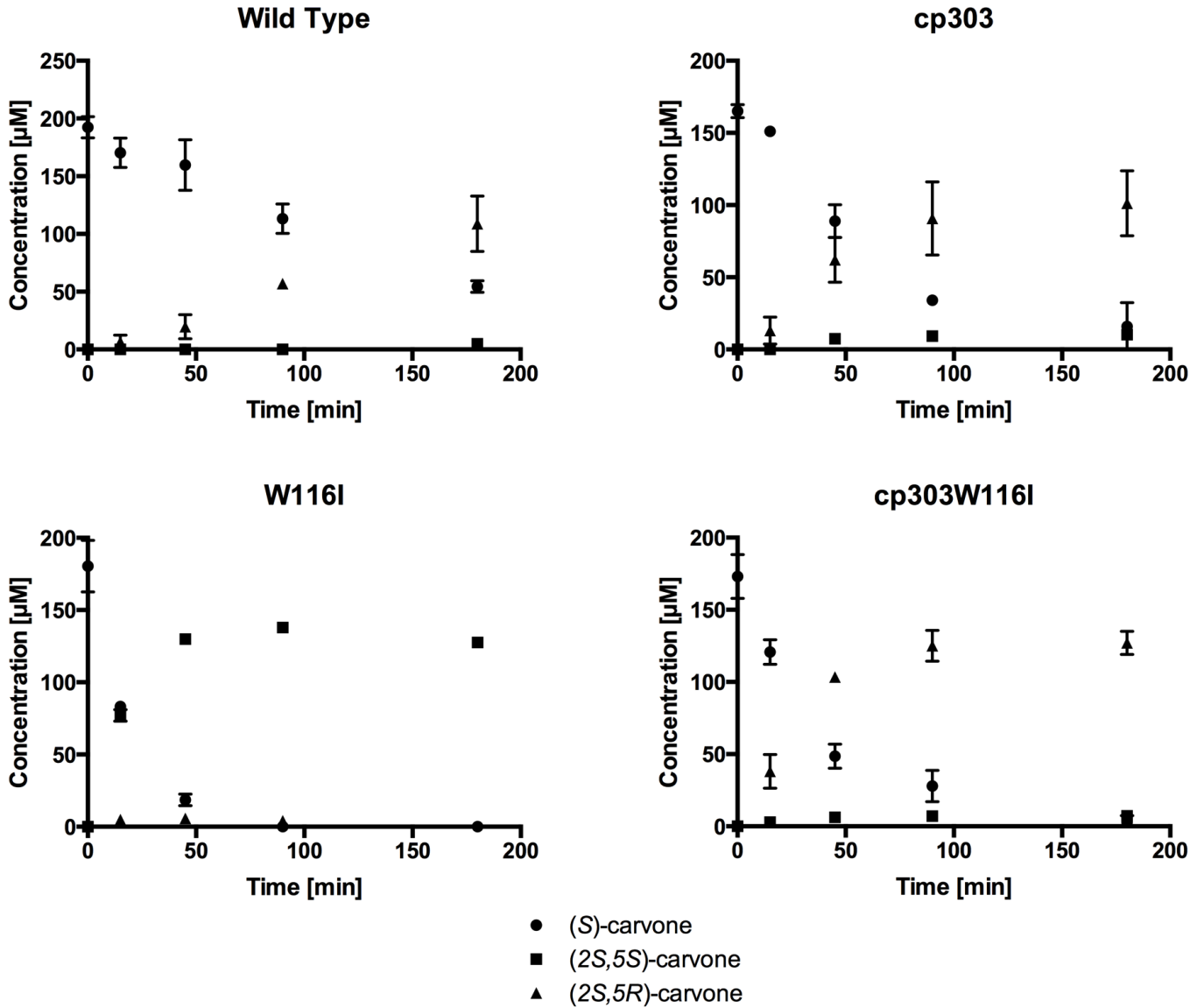
## 10.4 *Relatives concentrations and quantitative additional data*

### 10.4.1 *(S)-carvone*

Relative concentrations (average on three values) used for figure 16 for the conversion of (*S*)-carvone.

Enzyme	Time points [min]	( <i>S</i> )-carvone	(2 <i>R</i> ,5 <i>S</i> )-carvone	(2 <i>S</i> ,5 <i>S</i> )-carvone
<i>Wild Type</i>	0	100	0	0
	15	96.3	3.6	0
	45	88.6	11.3	0
	90	66	34	0
	180	33	64.5	3
<i>cp303</i>	0	100	0	0
	15	92	8	0
	45	56	39	4.5
	90	26	66.5	7
	180	13	79	8
<i>W116I</i>	0	100	0	0
	15	51.5	47.5	2
	45	12.5	84.5	3
	90	3.6	92.3	4
	180	1.3	95	3.6
<i>cp303W116I</i>	0	100	0	0
	15	78.5	19.5	0
	45	30.5	65.5	4
	90	17.5	78	5
	180	2	93	5

Quantitative data plotted against time for (*S*)-carvone.

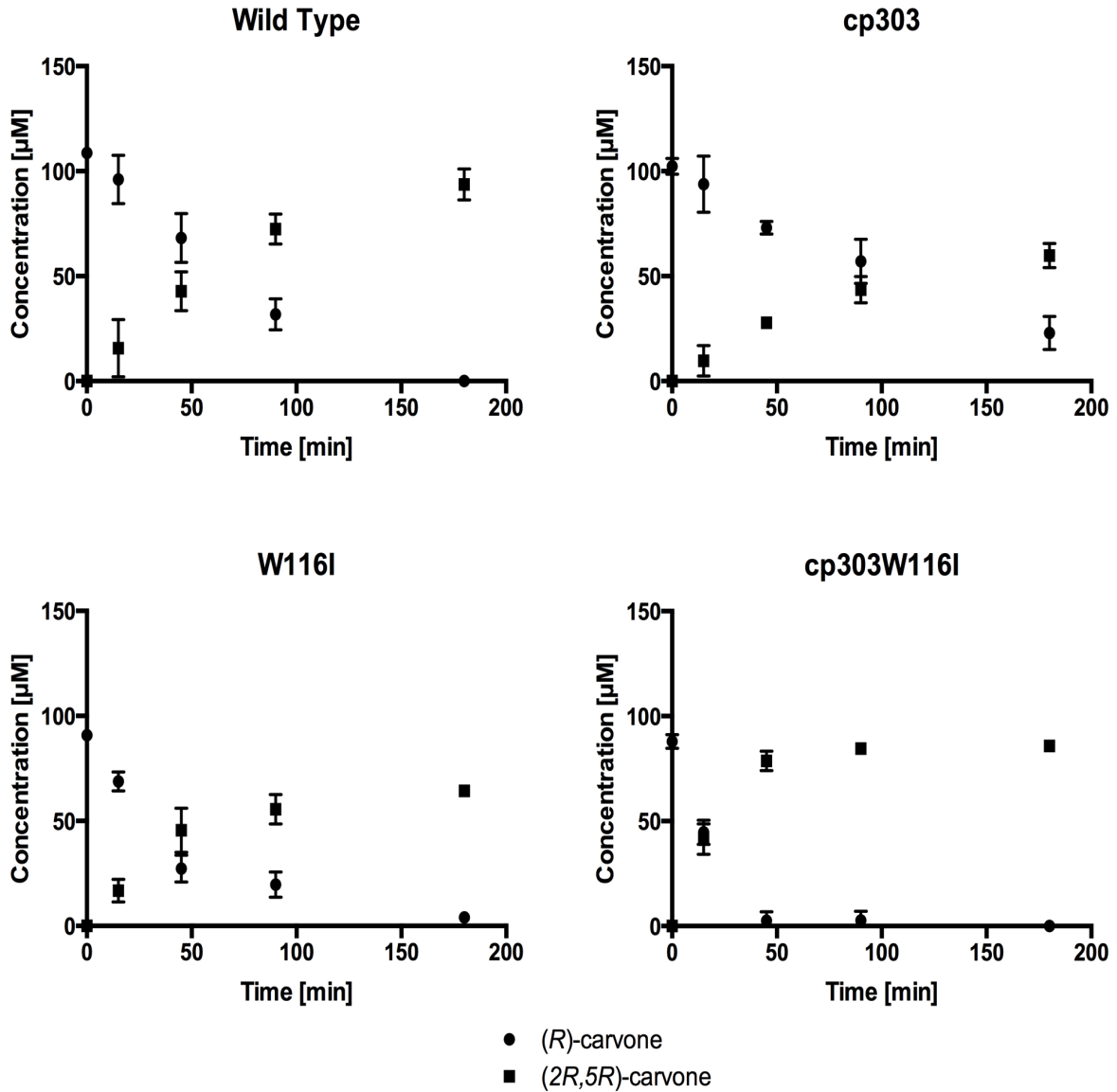


### 10.4.2 (*R*)-carvone

Relative concentrations (average on three values) used for figure 17 for the conversion of (*R*)-carvone.

Enzyme	Time points [min]	( <i>R</i> )-carvone	(2 <i>R</i> ,5 <i>R</i> )-carvone	(2 <i>R</i> ,5 <i>S</i> )-carvone
<i>Wild Type</i>	0	100	0	0
	15	86.5	13.5	0
	45	61.3	38.6	0
	90	30.3	69.6	0
	180	0	100	0
<i>cp303</i>	0	100	0	0
	15	90.3	9.6	0
	45	72.3	27.6	0
	90	56.3	43.6	0
	180	27.6	72.3	0
<i>W116I</i>	0	100	0	0
	15	80.3	19.6	0
	45	37.6	62.3	0
	90	26.3	73.6	0
	180	5.6	94.3	0
<i>cp303W116I</i>	0	100	0	0
	15	52	48	0
	45	3	97	0
	90	3	97	0
	180	0	100	0

Quantitative data plotted against time for (*R*)-carvone.

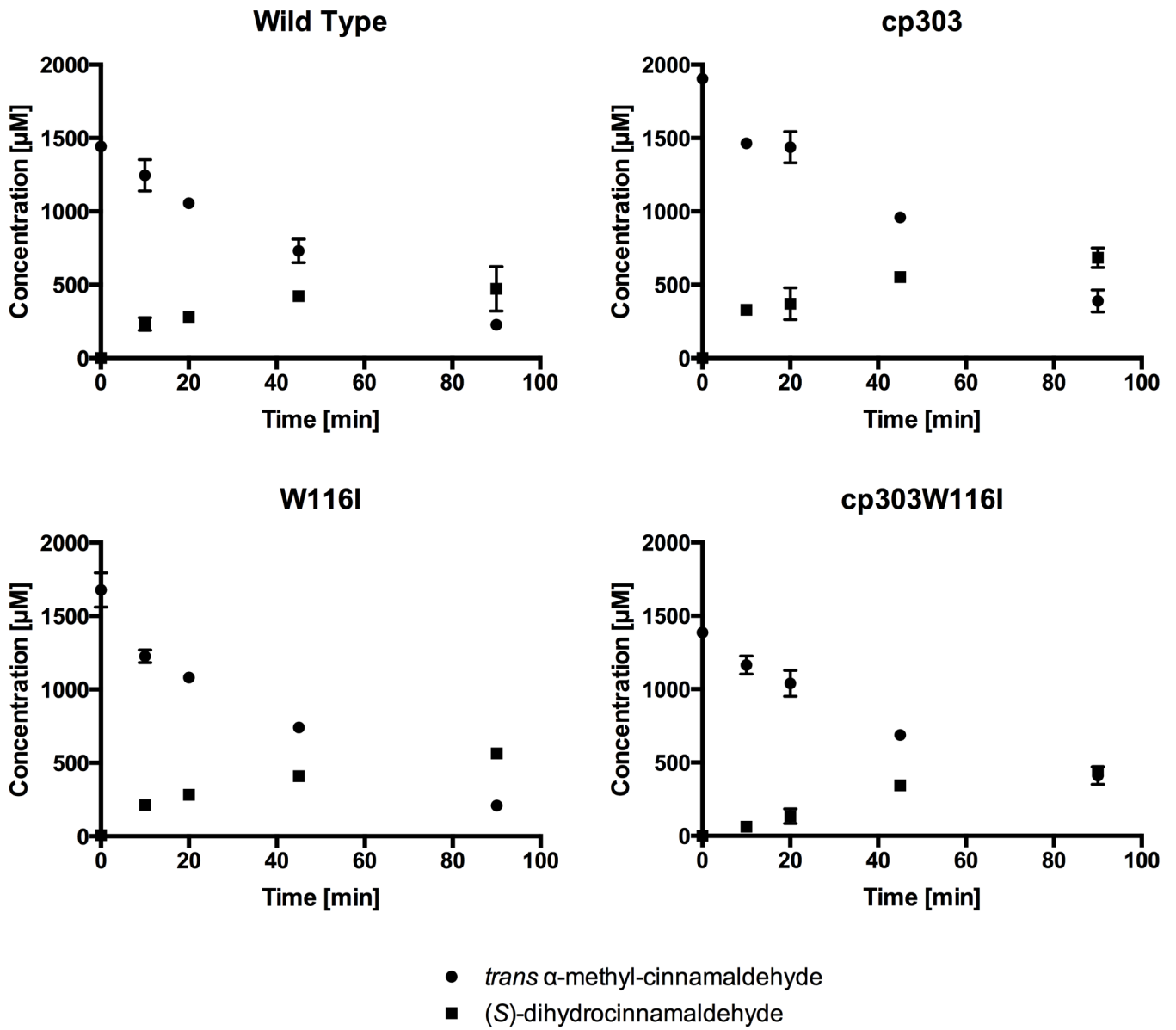


### 10.4.3 *Trans* $\alpha$ -methyl-cinnamaldehyde

Relative concentrations (average on three values) used for figure 20 for the conversion of *trans*  $\alpha$ -methyl-cinnamaldehyde.

Enzyme	Time points [min]	<i>trans</i> $\alpha$ -methyl-cinnamaldehyde	( <i>S</i> )-dihydrocinnamaldehyde
<i>Wild Type</i>	0	100	0
	10	91.6	8.3
	20	88	12
	45	76.6	23.3
	90	42.3	57.6
<i>cp303</i>	0	100	0
	10	90	10
	20	88.3	11.6
	45	77	23
	90	49	51
<i>W116I</i>	0	100	0
	10	92	8
	20	88.3	11.6
	45	77.6	22.3
	90	34	66
<i>cp303W116I</i>	0	100	0
	10	97.6	2.3
	20	94	6
	45	79	21
	90	61.5	38.5

Quantitative data plotted against time for *trans*  $\alpha$ -methyl-cinnamaldehyde.

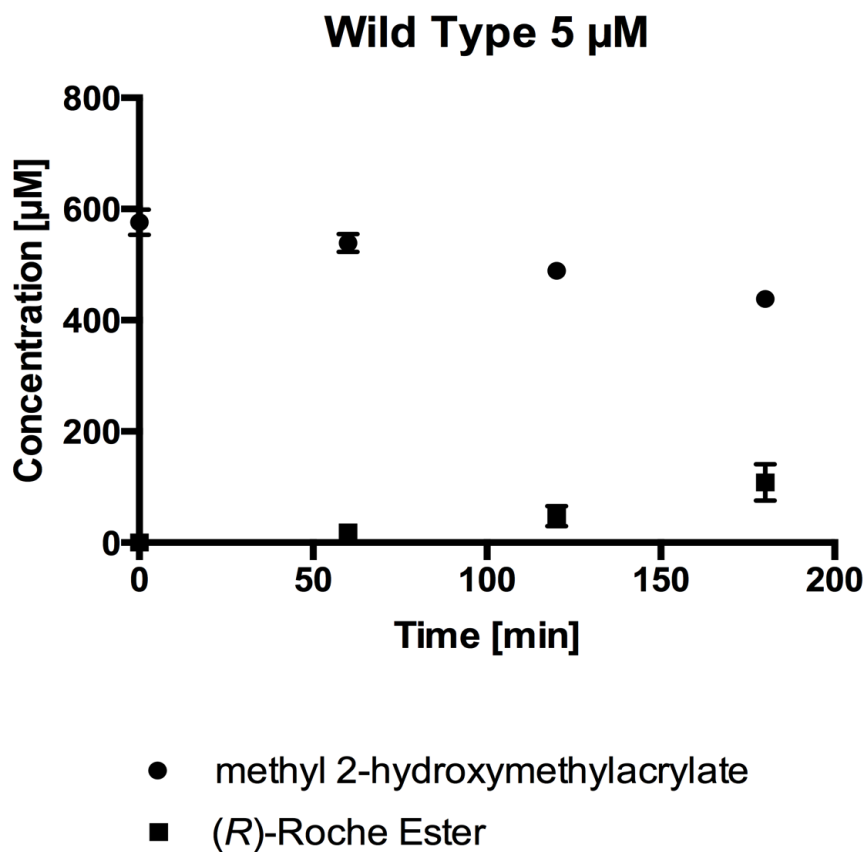


### 10.4.4 Methyl 2-hydroxymethylacrylate

Relative concentrations (average on three values) used for figure 26 for the conversion of methyl 2-hydroxymethylacrylate.

Enzyme	Time points [min]	methyl 2-hydroxymethylacrylate	(R)-'Roche Ester'
	0	100	0
<i>Wild Type</i>	60	97.6	2.3
	120	93.3	6.6
	180	84.6	15.3

Quantitative data plotted against time for methyl 2-hydroxymethylacrylate.

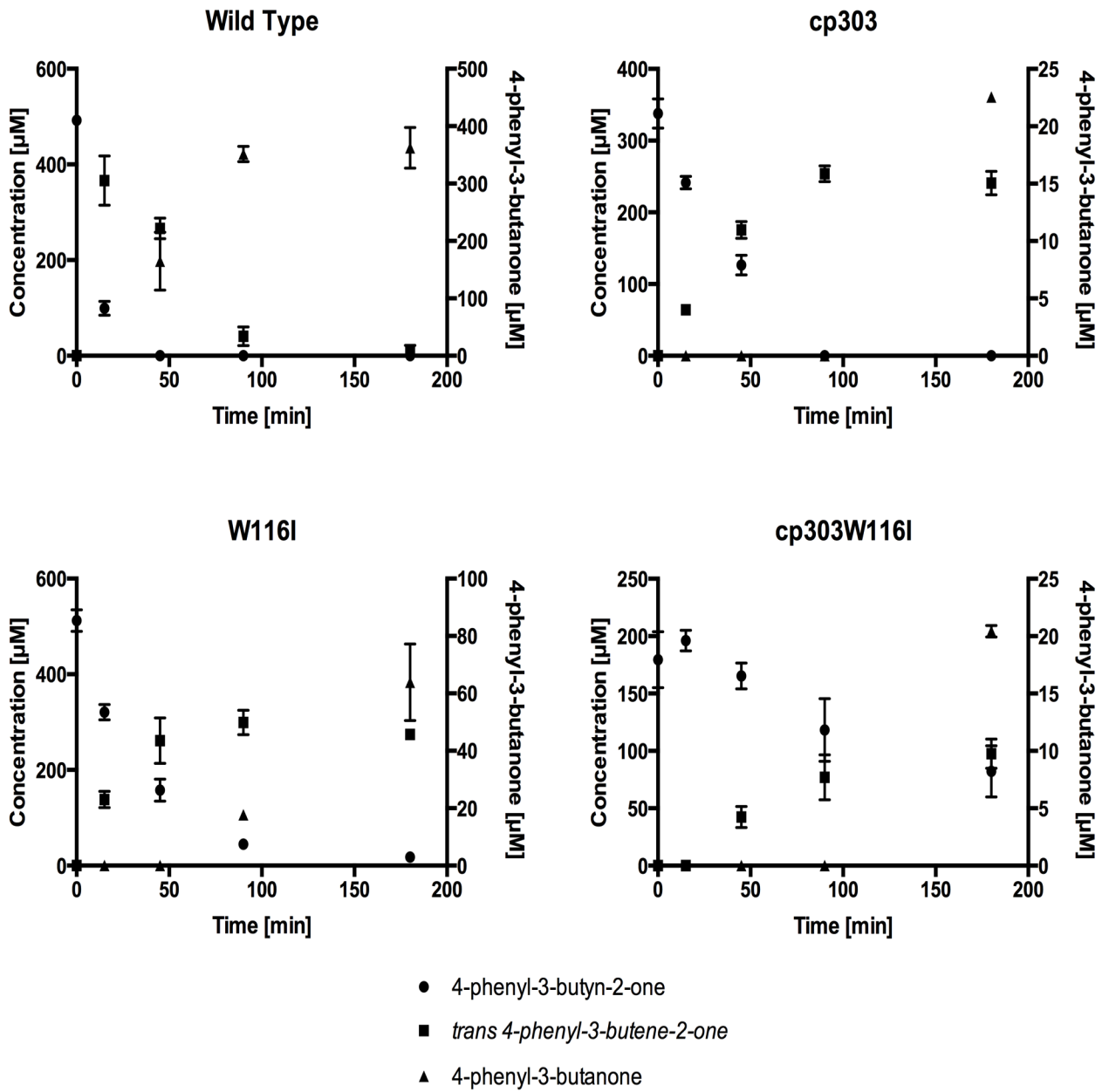


### 10.4.5 4-phenyl-3-butyn-2-one

Relative concentrations (average on three values) used for figure 29 for the conversion of 4-phenyl-3-butyn-2-one.

Enzyme	Time points [min]	4-phenyl-3-butyn-2-one	<i>trans</i> 4-phenyl-3-butene-2-one	4-phenyl-2-butanone
<i>Wild Type</i>	0	100	0	0
	15	21	77.6	2
	45	0	46.3	53.6
	90	0	4	96
	180	0	0.3	99.6
<i>cp303</i>	0	100	0	0
	15	83	17	0
	45	56.6	56.6	0
	90	0	84.3	15.6
	180	0	75	25
<i>W1161</i>	0	100	0	0
	15	73	27	0
	45	36.6	56.6	6.6
	90	8.5	70.5	20.5
	180	2.5	61	36.5
<i>cp303W1161</i>	0	100	0	0
	15	100	0	0
	45	85.3	14.6	0
	90	72	28	0
	180	41.5	58.5	0

Quantitative data plotted against time for 4-phenyl-3-butyn-2-one.

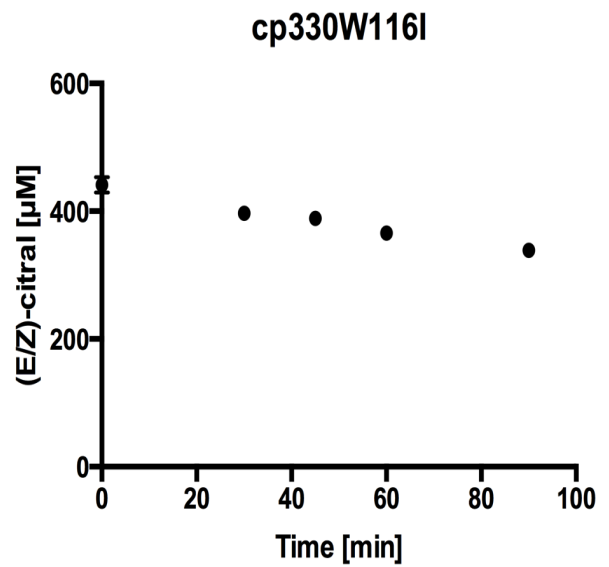
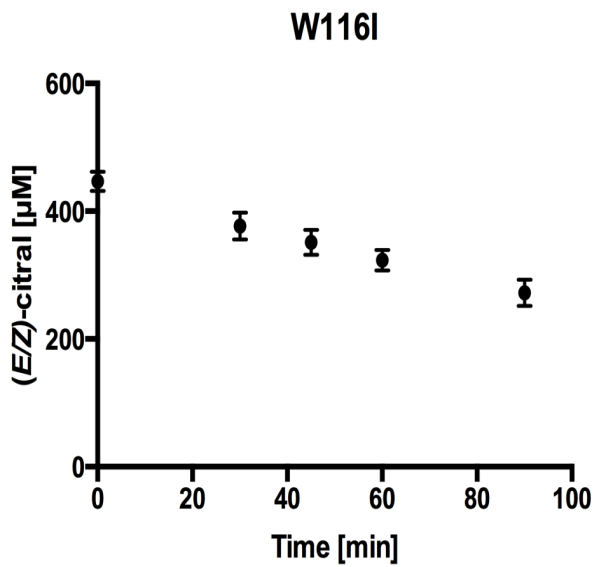
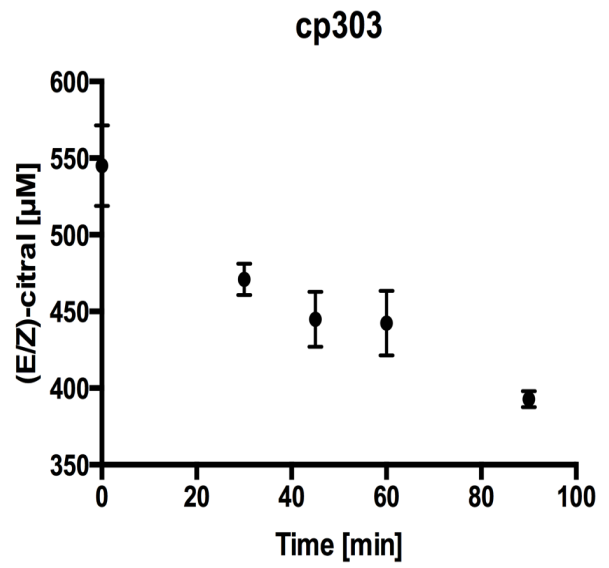
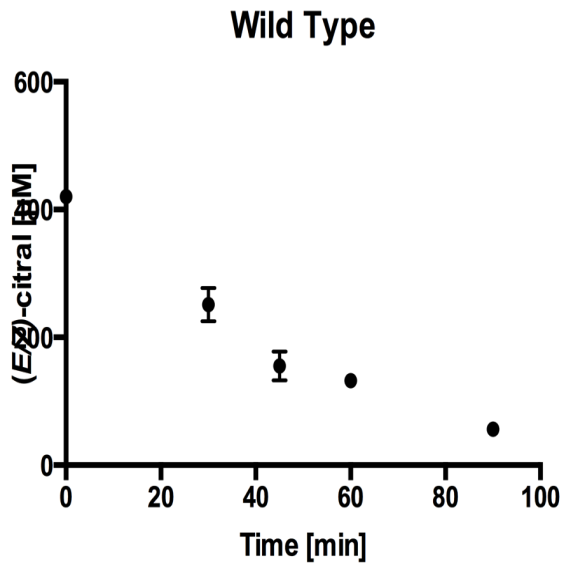


### 10.4.6 (E/Z)-citral

Relative concentrations (average on three values) used for figure 35 for the conversion of (E/Z)-citral.

Enzyme	Time points [min]	(E/Z)-citral	(S/R)-citronellal
<i>Wild Type</i>	0	100	0
	30	84.3	15.6
	45	71	29
	60	66.3	33.6
	90	35.6	64.3
<i>cp303</i>	0	100	0
	30	85.6	0
	45	81	0
	60	80.3	0
	90	71	0
<i>W116I</i>	0	100	0
	30	96.6	3.3
	45	95.6	4.3
	60	93.6	6.3
	90	87	13
<i>cp303W116I</i>	0	100	0
	30	93.3	0
	45	91.3	0
	60	86	0
	90	76	0

Quantitative data plotted against time for (*E/Z*)-citral.



## 10.5 Equipment pictures

### 10.5.1 Anion and Size exclusion Äkta module

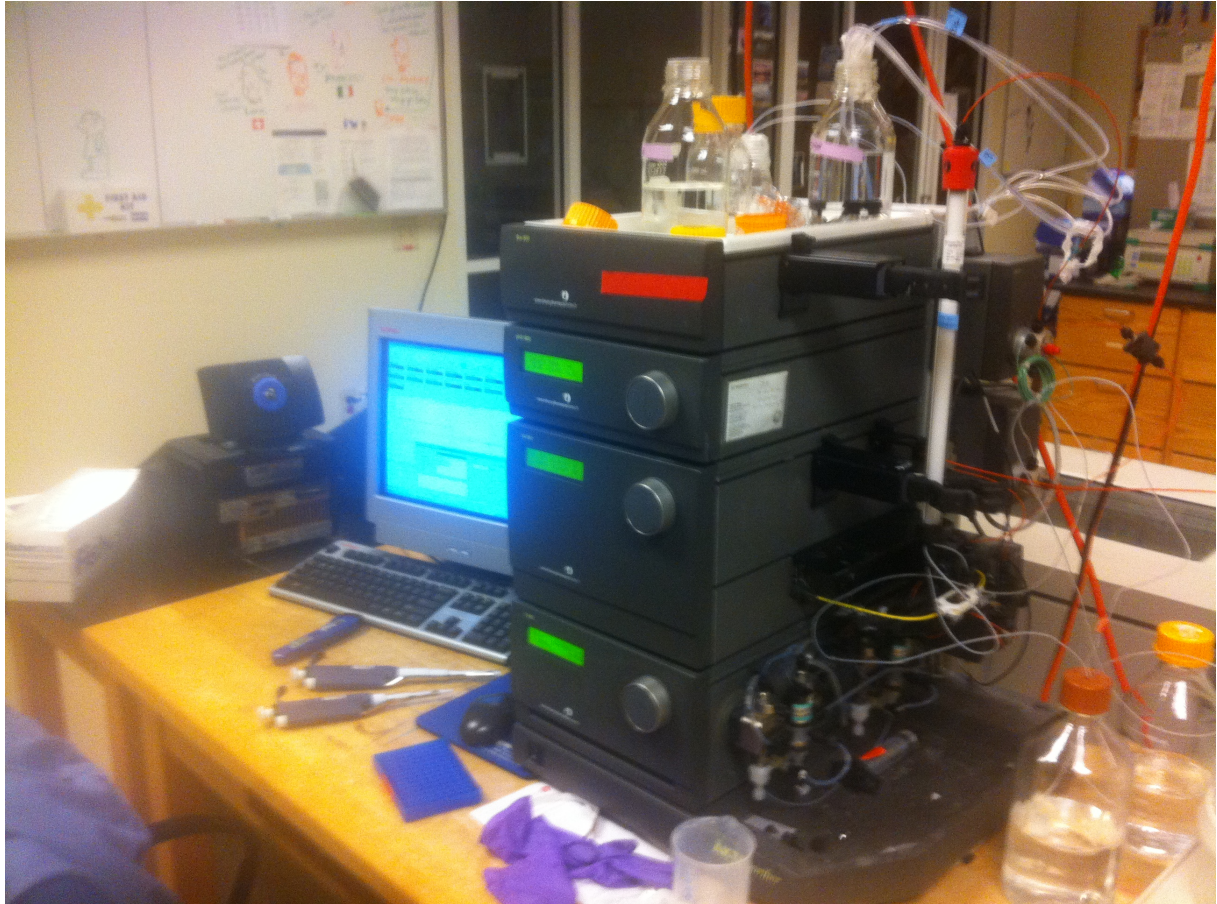


*Figure 42: Äkta purifier from Amersham pharmacia biotech.*

### 10.5.2 Gas Chromatography

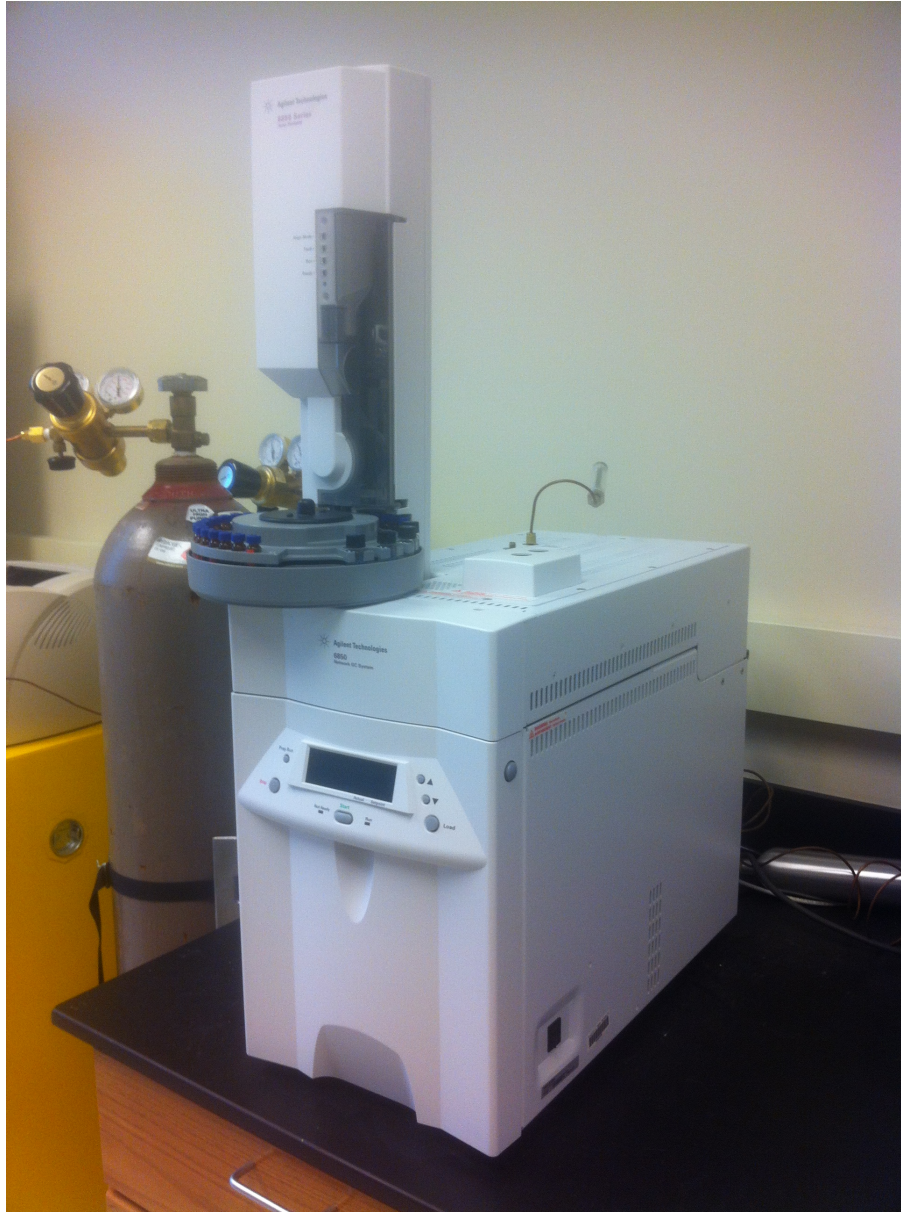


*Figure 43: Gas Chromatography apparel used for this work. Agilent 6850 Series.*

### 10.5.3 Anaerobical chamber



*Figure 44: Anaerobical chamber from Coy Laboratories.*